

SLA²P: Self-supervised Anomaly Detection with Adversarial Perturbation*

Yizhou Wang[†], Can Qin[†], Rongzhe Wei[‡], Yi Xu[†], Yue Bai[†] and Yun Fu[†]

[†] Northeastern University, [‡] Purdue University

wyzjack990122@gmail.com, {qin.ca, xu.yi, bai.yue}@northeastern.edu,
wei397@purdue.edu, yunfu@ece.neu.edu

Abstract

Anomaly detection is a fundamental yet challenging problem in machine learning due to the lack of label information. In this work, we propose a novel and powerful framework, dubbed as SLA²P, for unsupervised anomaly detection. After extracting representative embeddings from raw data, we apply random projections to the features and regard features transformed by different projections as belonging to distinct pseudo classes. We then train a classifier network on these transformed features to perform self-supervised learning. Next we add adversarial perturbation to the transformed features to decrease their softmax scores of the predicted labels and design anomaly scores based on the predictive uncertainties of the classifier on these perturbed features. Our motivation is that because of the relatively small number and the decentralized modes of anomalies, 1) the pseudo label classifier’s training concentrates more on learning the semantic information of normal data rather than anomalous data; 2) the transformed features of the normal data are more robust to the perturbations than those of the anomalies. Consequently, the perturbed transformed features of anomalies fail to be classified well and accordingly have lower anomaly scores than those of the normal samples. Extensive experiments on image, text and inherently tabular benchmark datasets back up our findings and indicate that SLA²P achieves state-of-the-art results on unsupervised anomaly detection tasks consistently.

1 Introduction

Anomalies, also known as outliers, are defined as “data instances that significantly deviate from the majority of data instances” (Pang et al., 2020a). Correspondingly, anomaly detection (AD) refers to the process of finding these anomalous data points out in a data-driven fashion, which has long been a fundamental problem in machine learning and has various real-world applications, including medical health (Min et al., 2017; Khan and Yairi, 2018), fraud detection (Adewumi and Akinyelu, 2017; Shen et al., 2007; Fu et al., 2016), cybersecurity (Tan et al., 2011; Kwon et al.,

*The code will be made publicly available after the acceptance of the paper for publication.

2019) and video surveillance (Chen et al., 2015; Sultani et al., 2018) etc. In view of whether and to what degree labels are available, anomaly detection tasks can be generally classified into three categories: 1) Supervised anomaly detection involves training models on a labeled dataset consisting of both inliers and outliers and then applying them to test data. 2) Semi-supervised anomaly detection (SSAD), or one-class classification, deals with the setting that the training dataset is only composed of normal data and the trained model is supposed to detect anomalous data in the testing phase. 3) Unsupervised anomaly detection (UAD), which is the most common and challenging case, obeys the condition that solely unlabeled data with both inliers and outliers are provided and the anomaly detection technique is required to be capable of detecting the outliers (Chandola et al., 2009). These three categories consider anomalies as points that are intrinsically from distinct classes from normal points'. Besides, there exists another type of AD called out-of-distribution (OOD) detection (Liang et al., 2018; Hendrycks et al., 2019; Hsu et al., 2020; Liu et al., 2020), which aims to distinguish samples that have disjoint distribution from training samples (usually from a different dataset).

We mainly focus on the unsupervised setting, i.e., UAD, which is most widely applicable because it is costly to obtain labels for AD in many real-world scenarios (Pang et al., 2020a; Chalapathy and Chawla, 2019; Chandola et al., 2007). UAD has wide-range applications in practice, including large-scale dataset construction, website management and news management etc. We must clarify that in some literatures, the so-called "unsupervised anomaly detection" actually refers to SSAD (e.g., (Somepalli et al., 2020; Kwon et al., 2020; Venkataramanan et al., 2019)) or OOD (e.g., (Schirrmeyer et al., 2020)) by our definition, which is beyond the scope of this paper.

In this work, we introduce a novel SeLf-supervised framework for unsupervised Anomaly Detection using Adversarial Perturbation, which we name as SLA^2P . With the extracted embeddings from unlabeled raw data, we project them into different subspaces by multiplying random matrices. Despite having no explicit idea of the subspaces, we deem the transformation to be digging various unknown aspects of latent information of the data. Then we train a deep neural network (DNN) classifier on the transformed features in order to distinguish which subspace they are projected into. The training process of the classifier is equipped with early stopping technique to prevent overfitting and the reason behind this is that outliers fail to be trained well owing to their smaller population size and more various modes. The trained classifier is supposed to mostly learn useful information concerning characteristics of the normal data, hence its predictive uncertainties can be utilized to design anomaly scores, with anomalies having more uniform predictions while normal instances having sharper predictions. Such prediction distribution disparities can be further amplified by adding adversarial perturbations to these transformed features. The aim of the perturbations is to decrease the softmax scores of the predicted labels of the transformed features by the classifier. The practice boosts UAD performance empirically, and we are not aware of any other analogous approach in the anomaly detection field. To summarize, our contributions are four-fold:

- We propose a novel framework SLA²P for UAD, which can be applied to image, text and inherently tabular datasets. Our approach is the first attempt to use **feature-level transformation** to create pretext classification task as surrogate supervision for UAD task .
- We investigate UAD task by involving **adversarial perturbation** technique in a **self-supervised** fashion to achieve considerable performance improvement.
- Our method achieves state-of-the-art (SOTA) results on 7 challenging datasets, surpassing the current best methods by a considerable margin. Besides, it is **highly robust** and can maintain excellent detection performance under particularly high or small anomaly ratios.
- We further theoretically analyze SLA²P by illustrating the “**similarity-preserving**” property of random projections, which bridges image-level and feature-level transformation based self-supervised methods.

2 Related Works

Unsupervised anomaly detection. Traditional methods for UAD are mostly based on classic unsupervised learning tools, including density estimation methods (Breunig et al., 2000; Yang et al., 2009; Kim and Scott, 2012), clustering methods (Ester et al., 1996; He et al., 2003), dimension reduction methods (Shyu et al., 2003; Paffenroth et al., 2018) and one-class support vector machine methods (Schölkopf et al., 2000; Amer et al., 2013). Thanks to the marvelous representation ability of DNNs, many reconstruction-based methods using DNNs are developed for UAD in recent years. They mainly employ deep generative models (Zenati et al., 2018; Perera et al., 2019; Lai et al., 2020b) or autoencoders (AE) (Chen et al., 2017; Pidhorskyi et al., 2018; Abati et al., 2019) to reconstruct data and determine abnormality of data via its reconstruction error. For instance, DAGMM (Zong et al., 2018) feed the latent representations of the AE into a gaussian mixture model and jointly optimize them. RSRAE (Lai et al., 2020a) incorporates a robust PCA layer (Lerman and Maunu, 2018) into deep AEs, which is designed to project normal data into their subspace while leaving anomalies out. Sound as these carefully designed architectures seem, it is inevitable that such reconstruction-based methods focus more on low-level or element-wise error rather than high-level semantic information, as pointed out by Wang et al. (2019).

Anomaly detection with pretrained networks. Transferring discriminative embeddings of pretrained nets to AD has been widely studied and achieved great success (Sabokrou et al., 2018; Rippel et al., 2020; Ruff et al., 2020). (Andrews et al., 2016) shows that transfer-representation-learning approaches offer viable representations for AD tasks without prior knowledge of the data. Methods in (Kumagai et al., 2019; Vercauysen et al., 2020) improve AD performance on target domains via transferring information of related domains. Burlina et al. (2019) employs pretrained VGGNets (Simonyan and Zisserman, 2015) to perform novelty detection. Recently DNNs

pretrained on ImageNet have been used to extract features for unsupervised anomaly detection and segmentation on images (Bergmann et al., 2019, 2020; Bergman et al., 2020; Venkataramanan et al., 2019) and videos (Nazare et al., 2018; Pang et al., 2020b).

Self-supervised learning. Self-supervised Learning (SSL) has been an increasingly prevailing unsupervised learning method. SSL methods learn representations via designing a pretext task between inputs and self-defined signals (Bojanowski and Joulin, 2017; Gidaris et al., 2018) or contrastive learning (Oord et al., 2018; Chen et al., 2020). Employing SSL techniques to assist semi-supervised AD has shown promising results recently (Golan and El-Yaniv, 2018; Bergman and Hoshen, 2020; Tack et al., 2020; Schwag et al., 2021). In UAD task, E³Outlier (Wang et al., 2019) trains a discriminative DNN via SSL and use the network outputs of the DNN to design anomaly scores. Nevertheless, such practice can only be applied to image data and require manually pre-defined transformations. By contrast, our method can be applied to both image and tabular data, and in our framework random transformations are able to exhibit promising performance.

Input perturbation. Input adversarial perturbation technique is first proposed by (Goodfellow et al., 2014) to generate adversarial data samples to fool the classifier. In OOD detection, several works utilize the opposite perturbation to the input raw data using the gradient of the maximum softmax score of the predicted label attained from pretrained network (Liang et al., 2018; Hsu et al., 2020). Lee et al. (2018) add perturbation to increase the proposed Mahalanobis distance-based confidence score for OOD detection. In anomaly/outlier detection area, there are few efforts in utilizing input perturbations to enhance AD performance as we can not directly utilize the softmax outputs of some pretrained network. To the best of our knowledge, we make the first attempt to wisely combine perturbation technique with self-supervised learning to address AD problems.

3 Problem Statement

We consider data space $\mathcal{X} \subset \mathbb{R}^d$ and we are given an unlabeled dataset $X \subset \mathcal{X}$. X contains both normal data (inliers) X_{in} of size n and anomalous data (outliers) X_{out} of size np , where $0 < p < 1$ is the anomaly rate defined as the ratio of anomalies to normal data. The essential objective of UAD is to design a universal indicator function $I(\mathbf{x}) : \mathcal{X} \rightarrow \{0, 1\}$ such that $I(\mathbf{x}) = 1$ for $\mathbf{x} \in X_{\text{in}}$ and $I(\mathbf{x}) = 0$ for $\mathbf{x} \in X_{\text{out}}$. However, directly pursuing such function is hard and inefficient, as there is a trade-off between type-I error (rate of normal samples which are classified as anomalies) and type-II error (rate of anomalous samples that are classified as normal) (Golan and El-Yaniv, 2018). The standard practice to deal with this problem is to instead design a scoring function $S(\mathbf{x}) : \mathcal{X} \rightarrow \mathbb{R}$ s.t. higher scores indicate more normality while lower scores indicate more anomaly.

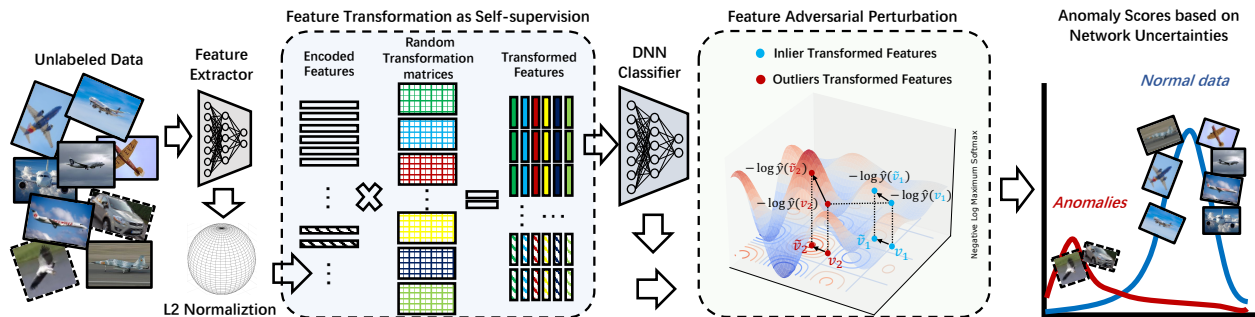


Figure 1: Overview of our proposed framework SLA^2P on image data. Given unlabeled image data with both inliers and outliers, we first extract representative features from raw data and normalize them into a unit sphere vector space (features of anomalies are shaded). We then apply random projections to the embeddings by multiplying matrices sampled randomly from standard normal distribution. Transformations by different matrices give rise to pseudo labels, on which we train a DNN classifier. Next we adversarially perturb the transformed samples using the gradients of the softmax scores of the predicted labels of the classifier. Finally, the anomaly scores are generated leveraging the predictive uncertainty estimates of the network on the perturbed transformed features. Best viewed in color.

4 Method

Our proposed framework SLA^2P is illustrated in Figure 1, which can be partitioned into three sub-processes.

4.1 Feature Extraction with L2 normalization

Given a raw datum \mathbf{x} , we employ a feature extractor \mathbf{f} to vectorize it into its discriminative embedding $\mathbf{f}(\mathbf{x}) \in \mathbb{R}^d$. The choice of f depends on the data type. We use a pretrained DNN for images and standard text pre-processing methods for text data. For inherently tabular data, the raw data is qualified to serve as its embedding, i.e., choosing \mathbf{f} to be identity mapping is enough. The detailed setting for different datasets is elaborated in Sec. 6. After feature extraction, we apply L2 normalization to the embeddings:

$$\mathbf{v}(\mathbf{x}) = \frac{\mathbf{f}(\mathbf{x})}{\|\mathbf{f}(\mathbf{x})\|_2}.$$

L2 normalization projects the embeddings into a sphere in \mathbb{R}^d , which only reduces the feature dimension by one but eliminates the differences of magnitudes (norms) among the unlabeled data (Gu et al., 2020). Our idea is that anomalies differ from normal data in intrinsic and latent distribution, not magnitudes. Therefore the normalization step is supposed to help the subsequent modules of SLA^2P to concentrate on semantic level discrepancies and attenuate low-level variances between normal and anomalous data. Our theoretical argument also corroborates its

effectiveness in that the proof of our similarity perserving Theorem 1 requires the L2-norm of the processed vectors to be 1 (see Sec. 5 for more details).

4.2 Feature-level Self-supervised Learning

Motivation from geometric transformations of images. Geometric transformations as self-supervision have obtained tremendous success on image unsupervised learning tasks (Golan and El-Yaniv, 2018; Gidaris et al., 2018; Wang et al., 2019) and the core idea is that DNNs are considered to be able to excavate useful information of image data if they are able to recognize their transformed patterns (Gidaris et al., 2018). Nevertheless, the majority of data in machine learning tasks is in tabular form that does not possess the same structure as 2D images, and there are not in-hand “geometric transformations” for data in vector forms. In fact, geometric transformations are usually performed by applying affine transformations to homogeneous coordinates of images. Given a coordinate pair $(x, y)^\top$, it is firstly represented as a three-dimensional vector by adding an additional dimension with element 1. Then the new coordinates $(x', y')^\top$ are yielded by multiplying a transformation matrix:

$$\begin{pmatrix} x' \\ y' \\ 1 \end{pmatrix} = \begin{pmatrix} a & b & c \\ d & e & f \\ 0 & 0 & 1 \end{pmatrix} \begin{pmatrix} x \\ y \\ 1 \end{pmatrix}.$$

When $a = \cos \theta, b = \sin \theta, d = -\sin \theta, e = \cos \theta, c = f = 0$, the manipulation performs rotation by angle θ ; when $a = e = 1, b = d = 0, c = x_0, f = y_0$, it performs translating image along x axis by x_0 and along y axis by y_0 .

Spurred by this, we propose to extend such kind of transformation to vector form data via replacing the coordinate vector with the vectors themselves. In this way, we can perform transformations in the feature-level to conduct self-supervised learning. The designing of transformation matrix still remains a problem since a rotation matrix of vectors does not have the same meanings as a rotation matrix for image 2D coordinates. Fortunately, our experiments show that utilizing random matrices with each element i.i.d. sampled from standard normal distribution is enough to exhibit outstanding results. Next, we give a detailed description of our method of using random matrices for self-supervision.

Random matrix multiplications as surrogate supervision. Let the random projection matrix set $\mathcal{A} = \{\mathbf{A}^{(1)}, \mathbf{A}^{(2)}, \dots, \mathbf{A}^{(M)}\}$. For any $1 \leq m \leq M$, $\mathbf{A}^{(m)} = (a_{ij}) \in \mathbb{R}^{k \times d}$ ($k \ll d$) are independent and identically distributed (i.i.d.) sampled and the elements of the matrix are also i.i.d. sampled from standard normal distribution

$$a_{ij} \sim \mathcal{N}(0, 1).$$

We design the random transformation to be multiplying the aforementioned random matrices to data embeddings:

$$\mathbf{v}^{(m)} = \mathbf{A}^{(m)} \mathbf{v},$$

thereby we have generated a self-labeled data set

$$D_{\mathcal{A}} \triangleq \left\{ \left(\mathbf{v}^{(m)}(\mathbf{x}), m \right) \mid \mathbf{x} \in \mathcal{X}, \mathbf{A}^{(m)} \in \mathcal{A} \right\}.$$

Here we treat m as the pseudo label of $\mathbf{A}^{(m)}\mathbf{v}$, and hence we have a self-defined classification dataset with $mn(1+p)$ transformed features. The random projections not only project feature embeddings into different spaces, but also perform dimension reduction. We observe that a random matrix multiplication project one subspace or convex set in \mathbb{R}^d to another subspace or convex set in \mathbb{R}^k , as claimed in Proposition 1. Considering that extracted features of normal data tend to be in a certain subspace or convex set, Proposition 1 guarantees that the transformed features of normal data are still in one subspace or convex set.

Proposition 1. For any real matrix $\mathbf{A} \in \mathbb{R}^{k \times d}$, \mathcal{V} is a linear subspace in \mathbb{R}^d and \mathcal{U} is a convex set in \mathbb{R}^d , then $\mathbf{A}\mathcal{V}$ is a linear subspace in \mathbb{R}^k and $\mathbf{A}\mathcal{U}$ is a convex set in \mathbb{R}^k .

Training pseudo label classifier. It is straightforward that we can train a multi-class classifier C_{θ} with parameters θ on the self-labeled dataset, i.e., the classifier is supposed to classify the transformed features $\{\mathbf{v}^{(m)}(\mathbf{x}_i)\}$ into pseudo-class m for every $1 \leq m \leq M$. The loss function is standard cross-entropy loss. We denote the softmax output vector of C_{θ} as $\mathbf{y}(\cdot|\theta)$ with m th element $y^{(m)}(\cdot|\theta)$ and then our self-defined pretext task can be formulated as

$$\min_{\theta} \frac{1}{n(1+p)} \sum_{i=1}^{n(1+p)} \mathcal{L}(\mathbf{x}_i|\theta),$$

where

$$\begin{aligned} \mathcal{L}(\mathbf{x}_i|\theta) &= -\frac{1}{M} \sum_{m=1}^M \log \left(y^{(m)} \left(\mathbf{v}^{(m)}(\mathbf{x}_i) | \theta \right) \right) \\ &= -\frac{1}{M} \sum_{m=1}^M \log \left(y^{(m)} \left(\mathbf{A}^{(m)}\mathbf{v}(\mathbf{x}_i) | \theta \right) \right). \end{aligned}$$

During the training stage, we employ an early stopping technique to refrain from overfitting. We set a hyperparameter μ as classification accuracy threshold such that the training stops as soon as the classification accuracy of the classifier in the current batch reaches $\mu \in (0, 1)$. This strategy plays a vital role in our framework, since if the classifier C_{θ} can distinguish all the transformed data the anomalous data fail to be detected easily by the classification result.

4.3 Network Uncertainty Based Scoring with Adversarial Perturbation

We define our anomaly score function $S(\mathbf{x})$ based on the predictive uncertainties of the classifier C_{θ} . Our goal is to make normal data have higher scores than anomalies. Instead of using the training results of the original transformed samples like (Golan and El-Yaniv, 2018; Wang et al., 2019) did, we add adversarial perturbations to the transformed features before feeding them into C_{θ} .

Adversarial perturbation to the transformed features. We adversarially perturb the transformed features employing the gradient of the negative log softmax score of the predicted class of the trained classifier C_θ w.r.t. the input sample. Mathematically, for any $1 \leq m \leq M$ and \mathbf{x} , we let

$$\tilde{\mathbf{v}}^m(\mathbf{x}) = \mathbf{v}^{(m)}(\mathbf{x}) + \eta(-\nabla_{\mathbf{v}^{(m)}(\mathbf{x})} \log \hat{y}^{(m)}(\mathbf{x}|\boldsymbol{\theta})), \quad (1)$$

where $\hat{y}^{(m)}(\mathbf{x}|\boldsymbol{\theta}) = \max_i y^{(i)}(\mathbf{v}^{(m)}(\mathbf{x})|\boldsymbol{\theta})$, and η is the perturbation magnitude. Considering C_θ has been trained well on most transformed data samples, such practice aims to lower the softmax score of the pseudo class with the highest prediction probability, i.e., to make the projected features more difficult to classify. Note that our adversarial perturbation form is different from (Goodfellow et al., 2014) as we do not involve the pseudo labels when computing the gradient. Empirically, we discover that after such operation the anomaly scores of both inliers and outliers will decrease, but the inliers will be more robust to the perturbations than the outliers.

Negative Brier Score. Inspired by reconstruction-based AD methods (Chen et al., 2017; Zong et al., 2018; Lai et al., 2020a) which employ L2 distance error of reconstruction and input as score, we utilize Euclidean distance for scoring by considering the one-hot encoding of the correct label as ground truth in the classification problem:

$$S(\mathbf{x}) = -\frac{1}{M} \sum_{m=1}^M \left\| \mathbf{y}(\tilde{\mathbf{v}}^m(\mathbf{x})|\boldsymbol{\theta}) - \mathbf{e}_m \right\|_2^2,$$

where \mathbf{e}_m is the m -th canonical basis vector representing the label vector of m -th pseudo class. $-S(\mathbf{x})$ refers to the mean squared error of the prediction outputs of C_θ and ground truth one-hot pseudo labels, which actually corresponds to a classic proper score rule known as Brier Score (Brier et al., 1950). The ideal case is that the normal data to have lower error and accordingly higher anomaly score.

5 Theoretical Foundation of SLA²P

Random projections do not manifestly preserve semantic information of data, which contrasts with geometric transformations (e.g., a rotated or translated plane is still a plane, not a bird). Due to randomness, one may have no explicit idea of what subspace the features are projected into and whether the random transformations have an influence on the discrepancies among original features. Intriguingly, we find that as long as the dimension k is sufficiently large, the L2 distance and inner product of transformed embeddings, which are two effective measures of similarities between high-dimensional vectors, are roughly in proportion to their original values by a constant factor k .

Theorem 1 (Similarity-preserving Property). Given any fixed m and index pair of the unlabeled dataset (i, j) , for any positive numbers $0 < \epsilon < 1$ and $0 < \delta < 1$,

(1) when $k > \frac{4 \log \frac{2}{\delta}}{\epsilon^2 - \epsilon^3}$, we have with probability at least $1 - \delta$ over the random sampling of matrix $\mathbf{A}^{(m)}$,

$$(1 - \epsilon) \|\mathbf{v}_i - \mathbf{v}_j\|_2^2 \leq \frac{\|\mathbf{v}_i^{(m)} - \mathbf{v}_j^{(m)}\|_2^2}{k} \leq (1 + \epsilon) \|\mathbf{v}_i - \mathbf{v}_j\|_2^2,$$

(2) when $k > \frac{4 \log \frac{4}{\delta}}{\epsilon^2 - \epsilon^3}$, we have with probability at least $1 - \delta$ over the random sampling of matrix $\mathbf{A}^{(m)}$,

$$\mathbf{v}_i \cdot \mathbf{v}_j - \epsilon \leq \frac{\mathbf{v}_i^{(m)} \cdot \mathbf{v}_j^{(m)}}{k} \leq \mathbf{v}_i \cdot \mathbf{v}_j + \epsilon.$$

The proof of Theorem 1 is given in the supplementary. As stated in Theorem 1, random projections are likely to preserve the similarities among features, i.e., originally distant features (e.g., one normal and one anomalous instance) will still be comparatively distant and features originally closely distributed (e.g., normal data) tend to be near each other after projection. This lays the theoretical foundation of our SLA²P framework in that, although the transformations are random, they still preserve the structure and inner relationship of the data points, which is coherent with handcrafted geometric transformations for 2D image data.

6 Experiments

6.1 Datasets

To manifest the generality and flexibility of SLA²P, we empirically evaluate our framework on three image datasets and four tabular datasets. The image datasets are CIFAR-10 (Krizhevsky et al., 2009), CIFAR-100 (Krizhevsky et al., 2009) and Caltech 101 (Fei-Fei et al., 2004). The tabular datasets are composed of text datasets 20 Newsgroups (Lang, 1995), Reuters-21578¹ and inherently tabular datasets Arrhythmia and KDDCUP99 (Dua and Graff, 2017). For the image and text classification datasets, each class of data serves as inliers in turn, and the average result over all the classes is reported as the overall performance. The detailed descriptions are as follows.

CIFAR-10 is composed of 60,000 32×32 images of 10 classes, with 6,000 images per class. In each experiment, the inliers are 6,000 images from one class and the outliers are 6000 × p images randomly selected from the rest classes.

CIFAR-100 consists of 60,000 32×32 images labeled according to 100 distinct categories. The 100 categories are grouped into 20 superclasses, with 3,000 images per superclass. In each experiment, the inliers are 3,000 images from one superclass, and the outliers are 3000 × p images randomly chosen from the rest of superclasses.

Caltech 101 contains 9,146 images of 101 different classes. The size of each image is 300 × 200. Following the experiment setting of (Lai et al., 2020a), we select 11 classes that contain at least

¹<http://www.daviddlewis.com/resources/testcollections/reuters21578/>

100 images and randomly sample 100 out of them for each class. In each experiment, the inliers are 100 images from one certain class and the outliers are $100 \times p$ images selected from the rest 10 classes at random.

20 Newsgroups is a text classification dataset with roughly 20,000 newsgroup documents, partitioned nearly evenly across 20 newsgroups, i.e., classes. We randomly sample 360 documents per class. In each experiment, the inliers are 360 documents from a certain class, and the outliers are $360 \times p$ documents randomly chosen from the rest classes.

Reuters-21578 is also a text classification dataset containing 90 text categories with multi-labels. We choose the five largest classes with single labels and sample 360 documents for each class at random. In each experiment, the inliers are the documents from a fixed class, and $360 \times p$ outliers are sampled randomly from the remaining four classes.

Arrhythmia is a small-scale medical dataset containing attributes on the diagnosis of cardiac arrhythmia in patients. The dataset contains 16 classes. We construct the anomalous dataset using the smallest classes 3,4,5,7,8,9,14,15 and the normal set using the rest. There are 452 data instances in total, among which 66 are anomalies.

KDDCUP99 is a large-scale intrusion detection dataset. Following (Zong et al., 2018) we use the entire UCI 10% dataset, where the non-attack classes are treated as anomalies. There are 97278 abnormal instances and 396743 normal ones.

6.2 Experimental Setup

We compare SLA²P with six SOTA anomaly detection methods: IF (Liu et al., 2008), OCSVM (Schölkopf et al., 2000; Amer et al., 2013), DAGMM (Zong et al., 2018), E³Outlier (Wang et al., 2019), RSRAE (Lai et al., 2020a) and PANDA (Reiss et al., 2021). We adopt the commonly used Area under the Receiver Operating Characteristic curve (AUROC) and Area under the Precision-Recall curve (AUPR) as evaluation metric. For AUPR, we consider outliers as “positive” when computing. All the experiments, including baseline methods, are run 5 times independently using the same random seeds 0, 1, 2, 3, 4 for reproducibility and fair comparison and the averaged scores are reported in the main paper. The source code and more experimental details (including each single experiment result) are provided in the supplementary.

Setup of SLA²P. For image data, we use ResNets (He et al., 2016) pretrained on ImageNet without the last fully connected layer to extract embeddings. To match the image input shapes, we first resize raw images to 224×224 using Bilinear Interpolation and then feed it into the extractor network. For text data, we apply TFIDF transformer and Hashing-vector (Rajaraman and Ullman, 2011) sequentially to pre-process raw data into vectors, which is the same process as in (Lai et al., 2020a). For inherently tabular data, we directly use raw data vectors as the input. On Reuters dataset, we set $M = 512$ and $k = 128$ due to high dimensionality. On KDDCup99 dataset, we set $M = 64$ and $k = 128$ because of high computational burden. On the rest of the datasets, we

set $M = 256$ and $k = 256$. For the early stopping threshold, we set $\mu = 0.75$ for 20 Newsgroups, $\mu = 0.3$ for Reuters and $\mu = 0.6$ for all the rest datasets. We choose the perturbation magnitude as $\eta = 10$ for 20 Newsgroups, $\eta = 1e2$ for Reuters, $\eta = 1e4$ for CIFAR-100 and $\eta = 1e3$ for all the rest datasets. In fact, setting $\mu = 0.6$ and $\eta = 1e3$ is universally adequate for different UAD tasks and there is an implicit relationship between these two hyperparameters (see ablation study). Assuming the input dimension of classifier network is q , for all the experiments, the classifier network is a 3-layer fully connected network with structure FC($q, 2q$)-FC($2q, 4q$)-FC($4q, M$). Batch normalization (Ioffe and Szegedy, 2015) is applied to each layer and LeakyReLU (Xu et al., 2015) is employed as activation functions. We use Adam (Kingma and Ba, 2015) to optimize the classifier network parameters with learning rate $1e-3$ and weight decay $5e-4$.

Setup of baseline methods. Our experiments indicate that all the benchmark methods, except E³outlier (which directly manipulates images), works better using extracted representative embeddings as input than using raw data as input. Hence for fair comparison, we compare our method to the baseline methods with extracted features as input in the sequel. For the implementation of the benchmarks, we adapt the code from package scikit-learn (Pedregosa et al., 2011) for IF and OCSVM. We implemented DAGMM and E³Outlier using the code² from (Wang et al., 2019) with minimal modifications such that they are applicable to our datasets and adapt to our experimental protocol. RSRAE results are obtained running the official public code³. We adapt PANDA for UAD setting by setting the training set and the testing set to be the same with both inliers and outliers using the official public code⁴. All the data preprocessing processes follow the original papers.

6.3 Results

We report average AUROC and AUPR of all the methods on all the datasets. To exhibit the generality of our approach, we present its performance under varying anomaly ratios $p = 10\%, 30\%, 50\%$. We name our approach without adversarial perturbation as SLA and include its performance as well. Results on image datasets using pretrained ResNet-50 network are given in Tab. 1. The results using pretrained ResNet-101 are provided in the supplementary for completeness, where slightly better performances are achieved owing to the usage of deeper pretrained DNN extractor. We also summarize the results on text datasets and inherently tabular datasets in Tables 2 and 3 respectively.

Performance on image datasets. As indicated in Tab. 1, the performance of our two proposed methods, especially SLA²P, consistently outperform existing methods on all the image datasets,

²<https://github.com/demonzyj56/E3Outlier>

³<https://github.com/dmzou/RSRAE>

⁴<https://github.com/talreiss/PANDA>

Dataset	p	IF	OCSVM	DAGMM	E ³ Outlier	RSRAE	PANDA	SLA (ours)	SLA ² P (ours)
CIFAR-10	0.1	83.24 / 43.55	85.19 / 47.57	59.86 / 15.73	85.89 / 45.09	83.58 / 42.48	86.69 / 59.43	<u>90.81</u> / <u>59.46</u>	91.56 / 62.91
	0.3	79.36 / 56.95	79.52 / 56.69	67.04 / 37.81	80.58 / 58.53	75.05 / 50.90	83.63 / 64.20	<u>87.68</u> / 70.08	87.69 / <u>70.03</u>
	0.5	75.94 / 62.25	74.83 / 60.04	62.73 / 44.84	77.44 / 64.26	71.27 / 56.92	82.75 / 68.20	<u>84.64</u> / <u>73.25</u>	84.71 / 73.66
CIFAR-100	0.1	77.35 / 33.35	79.98 / 35.58	54.47 / 12.09	80.36 / 33.61	<u>89.21</u> / <u>55.94</u>	84.70 / 58.33	87.51 / 52.13	91.45 / 71.70
	0.3	73.90 / 49.65	74.86 / 49.62	56.78 / 29.59	78.60 / 53.15	<u>85.33</u> / <u>66.40</u>	82.32 / 64.21	85.03 / 66.39	85.48 / 69.29
	0.5	70.81 / 56.51	71.21 / 55.96	55.13 / 38.16	76.22 / 61.00	81.68 / 69.46	77.83 / 68.88	82.48 / 71.21	<u>81.98</u> / <u>70.76</u>
Caltech 101	0.1	89.88 / 59.72	92.98 / 67.16	72.61 / 34.02	90.72 / 62.29	94.28 / 74.44	96.32 / 80.39	<u>96.36</u> / <u>80.98</u>	96.42 / 81.12
	0.3	87.12 / 69.86	86.80 / 69.40	73.53 / 49.20	87.37 / 70.97	87.52 / 69.94	94.67 / 85.72	<u>95.09</u> / <u>86.17</u>	95.35 / 87.70
	0.5	84.29 / 72.97	81.67 / 69.82	69.14 / 53.70	84.82 / 73.93	82.59 / 71.78	<u>93.97</u> / <u>88.91</u>	93.57 / 87.73	96.26 / 94.31

Table 1: AUROC/AUPR (%) results on image datasets for UAD with ResNet-50 as the feature extractor. The best in bold and the second best underlined. The mean scores over 5 independent runs are reported.

Dataset	p	IF	OCSVM	DAGMM	RSRAE	SLA (ours)	SLA ² P (ours)
20 Newsgroups	0.1	56.45 / 15.09	82.04 / 43.82	54.84 / 12.76	89.03 / 49.79	<u>90.77</u> / <u>50.57</u>	93.20 / 71.77
	0.3	58.35 / 34.56	75.07 / 52.28	54.07 / 27.38	<u>88.86</u> / <u>68.61</u>	86.29 / 63.58	90.16 / 74.21
	0.5	57.00 / 43.77	71.33 / 58.49	51.94 / 35.93	86.73 / <u>73.55</u>	84.48 / 71.18	<u>86.55</u> / 78.13
Reuters-21578	0.1	59.30 / 18.74	90.95 / 61.69	65.07 / 22.33	92.44 / 64.44	<u>93.51</u> / <u>64.58</u>	95.77 / 81.40
	0.3	58.86 / 35.99	83.24 / 63.25	59.33 / 33.61	<u>88.70</u> / <u>73.07</u>	88.07 / 71.95	95.52 / 89.68
	0.5	55.85 / 42.10	74.88 / 62.36	62.01 / 46.54	<u>83.39</u> / <u>72.93</u>	82.87 / 72.64	86.09 / 79.92

Table 2: AUROC/AUPR (%) results on text datasets for UAD. The mean scores over 5 independent runs are reported.

including CIFAR-10 and CIFAR-100, which are abidingly considered the most challenging benchmark datasets for UAD (Wang et al., 2019). In addition, SLA²P is robust to the anomaly ratio and can still attain exceptional performance when p is large, with AUROC 84.71% on CIFAR-10, 82.48% on CIFAR-100 and 96.26% on Caltech 101 when the number of anomalies reaches half the number of normal samples. This is commendable as when the number of anomalies increase, no matter what UAD method is used, it is inevitable that the adverse effect of the training of outliers to the training of inliers will increase accordingly (Lai et al., 2020a,b).

Performance on tabular datasets. Besides image datasets, our framework is also able to exhibit superior performance on tabular datasets as demonstrated in Tables 2 and 3. SLA²P achieves SOTA results on 20 Newsgroups, significantly outperforming current SOTA RSRAE by 3%-4% in AUROC and around 10% in AUPR for different anomaly ratios. On Reuters, our method works much better than current SOTA, with up to 6.8% gain in AUROC and 16.6% gain in AUPR when $p = 0.3$ over RSRAE. On inherently tabular datasets, SLA²P exhibits dominating performance with over 40% AUPR gain on Arrhythmia, over 20% AUPR gain on KDDCUP99, and the AUROCs and AUPRs of these two classical datasets all exceed 90%. The extraordinarily excellent performance

	Arrhythmia		KDDCUP99	
	AUROC (%)	AUPR (%)	AUROC (%)	AUPR (%)
IF	79.78 \pm 0.93	46.29 \pm 1.30	92.72 \pm 1.17	69.06 \pm 3.91
OCSVM	79.47 \pm 0.00	47.75 \pm 0.00	51.98 \pm 0.00	43.23 \pm 0.00
DAGMM	67.16 \pm 4.14	30.68 \pm 1.98	77.55 \pm 5.90	47.28 \pm 5.80
RSRAE	80.31 \pm 2.89	42.03 \pm 2.84	60.09 \pm 2.30	27.36 \pm 1.22
SLA (ours)	79.85 \pm 0.69	46.78 \pm 1.22	97.00 \pm 0.46	88.89 \pm 0.92
SLA ² P (ours)	98.93\pm0.08	90.59\pm0.66	97.59\pm0.34	90.59\pm0.86

Table 3: UAD performance on inherently tabular datasets.

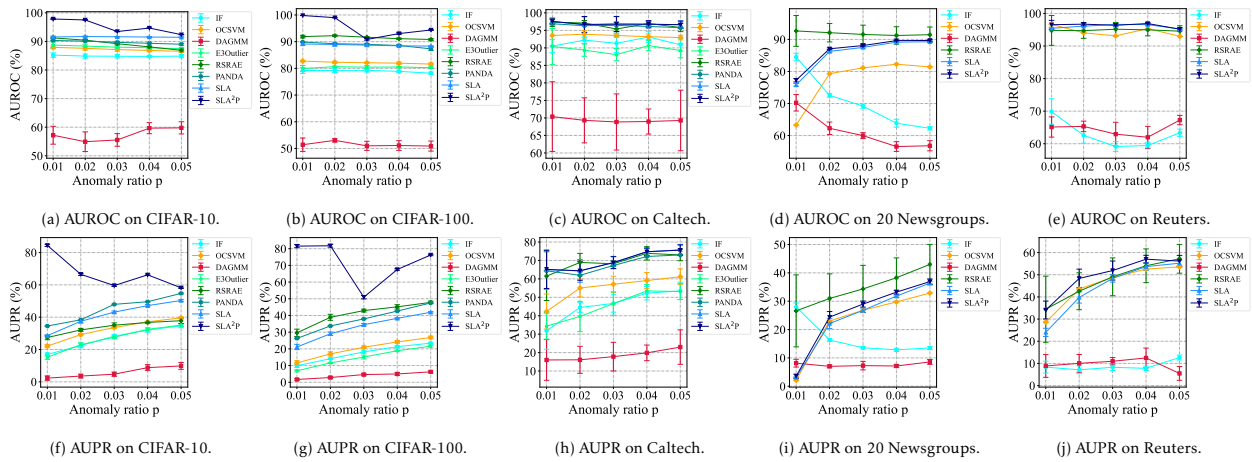


Figure 2: AUROC and AUPR scores with standard deviation bars when the anomaly ratio is tiny. Best viewed in color.

of SLA²P on the large-scale dataset KDDCUP99 reveals its practicality .

Performance under tiny anomaly ratios. The anomaly ratio can be extremely small in some UAD tasks and circumstances. Therefore we further compare our methods to the baseline methods when the anomaly rates are tiny: $p = 1\%, 2\%, 3\%, 4\%, 5\%$. Clearly seen from Fig. 2, our SLA²P still achieves favorable performance compared to other baseline methods. For all the aforementioned image and text datasets except 20 Newsgroups, SLA²P dominates in AUROC and AUPR with minimal numerical deviations. Furthermore, as demonstrated by the steadiness of the SLA²P curve in Fig. 2, SLA²P is remarkably stable with the alternation of p , especially in AUROC, despite the fact that we require sampling random matrices in our pipeline.

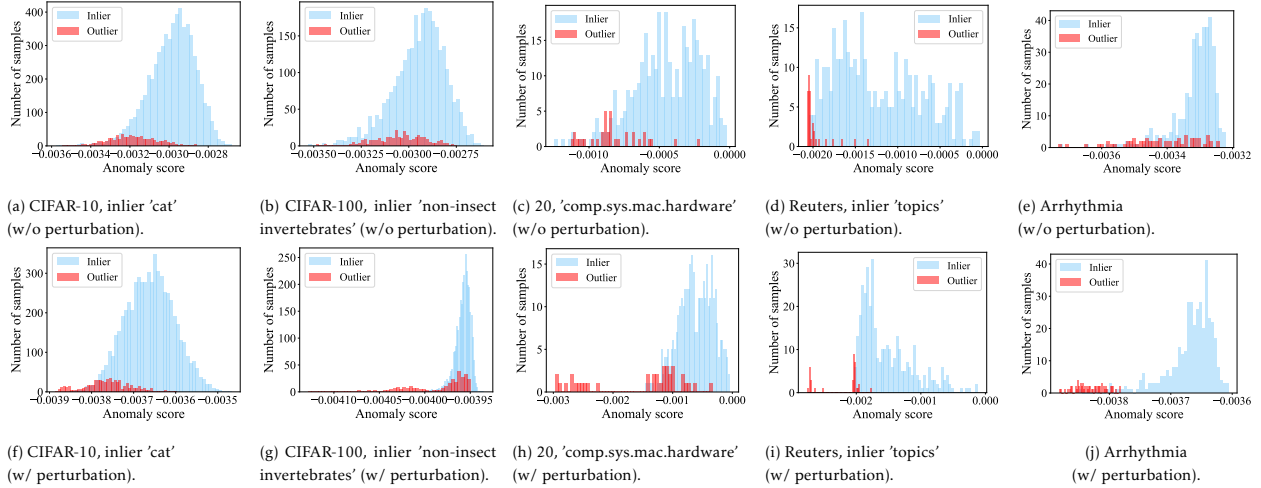


Figure 3: Distribution visualization of the anomaly scores before and after adversarial perturbation of our framework. Best viewed in color.

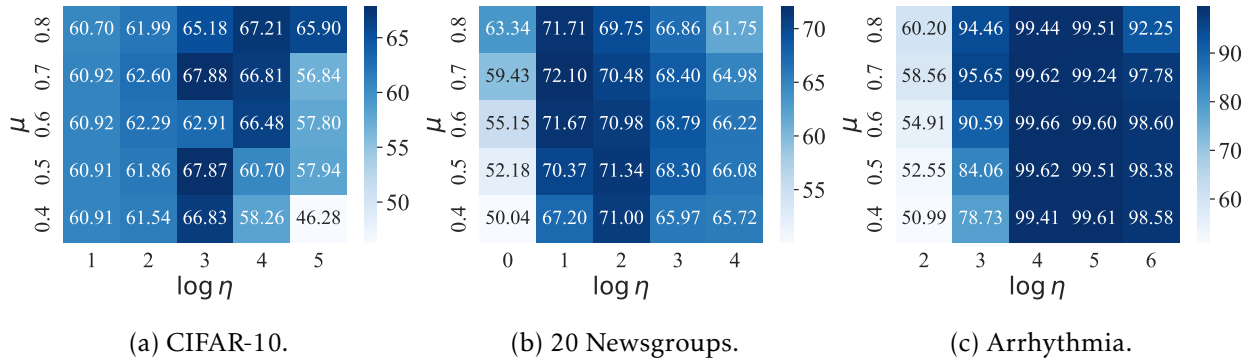


Figure 4: AUPR heatmap of our SLA^2P . Best viewed in color.

6.4 Ablation Study and Sensitivity Analysis

Effect of adversarial perturbation. To further demonstrate the function of the adversarial perturbations on the transformed features, we plot the anomaly score distributions before and after the perturbations. We choose experiments with inlier class 'cat' of CIFAR-10, 'non-insect invertebrates' of CIFAR-100, 'comp.sys.mac.hardware' of 20 Newsgrroups, 'topics' of Reuters. We also comprise Arrhythmia experiment. As shown in Fig. 3, despite our self-supervised SLA framework, there still exist outliers whose anomaly scores interlaces with those of inliers. In contrast, after the perturbation, the scores of both normal and anomalous data decreases but those of the inliers are more robust to the perturbations, making the anomalies more separable.

Relationship between μ and η . We provide fine-grained AUPR results when $p = 0.1$ on CIFAR-10, 20 Newsgrroups and Arrhythmia tuning $\mu \in \{0.4, 0.5, 0.6, 0.7, 0.8\}$ and η in log scale. As illustrated in Fig. 4, SLA^2P is highly robust w.r.t. the early stopping threshold μ and the perturbation

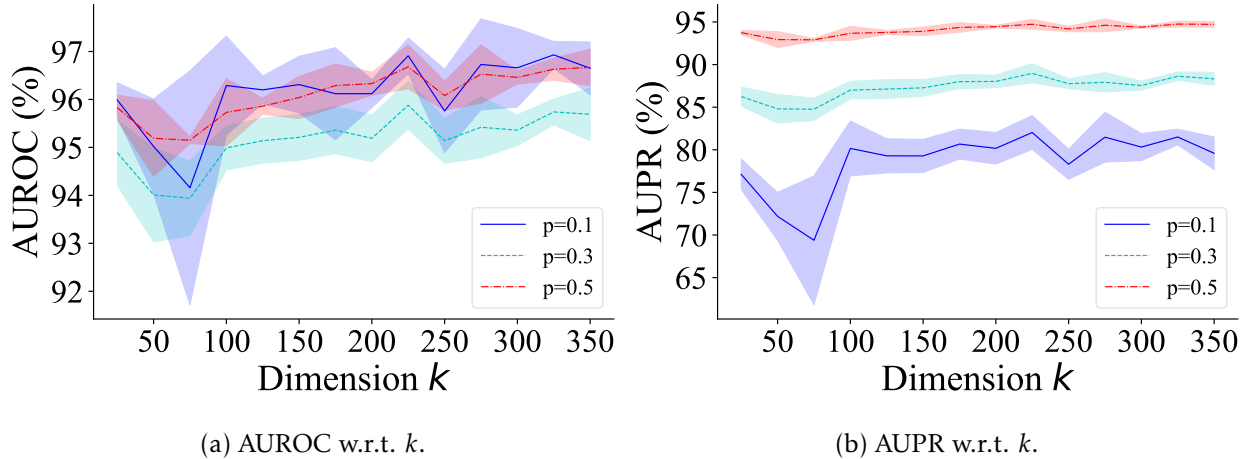


Figure 5: UAD performance on Caltech 101 with varying k of our proposed SLA²P method. Best viewed in color.

magnitude η . There is a wide range of hyperparameter permutations that make the AUPR score of SLA²P over 60% on CIFAR-10, over 55% on 20 Newsgroups and over 50% on Arrhythmia (all better than current SOTA baselines). Also, within the range of the hyperparameter values exhibiting competitive AD performance, higher μ typically requires larger η to guarantee satisfactory detection performance. This makes sense by intuition as the more transformed samples are classified well, the larger the stepsize of the perturbations should be to separate the anomalies out.

Robustness to transformed dimension k . We investigate the robustness of AD performance of SLA²P to the transformation matrix dimension k . We conduct ablation study on Caltech 101 dataset with k varying in the interval $[25, 350]$. The experiment is repeated for 5 times independently and the AUROC and AUPR curve w.r.t. dimension k are depicted in Fig. 5. From the figure we can draw the conclusion that UAD performance of SLA²P is generally robust w.r.t. k with moderate growth when k increases and the growth tends to be flatten out when k becomes comparatively larger. This phenomenon may be elucidated by Theorem 1 as k needs to be large enough to preserve the similarities between transformed features with high probability.

7 Conclusion

This paper proposes a novel framework, SLA²P, for unsupervised anomaly detection. We employ random projections as a feature-level self-supervised approach and incorporate adversarial perturbation into it to design discriminative anomaly scores. We further justify SLA²P’s effectiveness both theoretically and empirically. We hope this work may also shed light to pretext task based perturbation techniques for other unsupervised learning problems.

References

- ABATI, D., PORRELLO, A., CALDERARA, S. and CUCCHIARA, R. (2019). Latent space autoregression for novelty detection. In *CVPR*.
- ADEWUMI, A. O. and AKINYELU, A. A. (2017). A survey of machine-learning and nature-inspired based credit card fraud detection techniques. *International Journal of System Assurance Engineering and Management*.
- AMER, M., GOLDSTEIN, M. and ABDENNADHER, S. (2013). Enhancing one-class support vector machines for unsupervised anomaly detection. In *Proceedings of the ACM SIGKDD workshop on outlier detection and description*.
- ANDREWS, J., TANAY, T., MORTON, E. J. and GRIFFIN, L. D. (2016). Transfer representation-learning for anomaly detection. *JMLR*.
- ARRIAGA, R. I. and VEMPALA, S. (1999). An algorithmic theory of learning: Robust concepts and random projection. In *40th Annual Symposium on Foundations of Computer Science (Cat. No. 99CB37039)*.
- BERGMAN, L., COHEN, N. and HOSHEN, Y. (2020). Deep nearest neighbor anomaly detection. *arXiv preprint arXiv:2002.10445*.
- BERGMAN, L. and HOSHEN, Y. (2020). Classification-based anomaly detection for general data. In *ICLR*.
- BERGMANN, P., FAUSER, M., SATTLEGGER, D. and STEGER, C. (2019). Mvtec AD - A comprehensive real-world dataset for unsupervised anomaly detection. In *CVPR*.
- BERGMANN, P., FAUSER, M., SATTLEGGER, D. and STEGER, C. (2020). Uninformed students: Student-teacher anomaly detection with discriminative latent embeddings. In *CVPR*.
- BOJANOWSKI, P. and JOULIN, A. (2017). Unsupervised learning by predicting noise. In *ICML*.
- BREUNIG, M. M., KRIEGEL, H.-P., NG, R. T. and SANDER, J. (2000). Lof: identifying density-based local outliers. In *Proceedings of the 2000 ACM SIGMOD international conference on Management of data*.
- BRIER, G. W. ET AL. (1950). Verification of forecasts expressed in terms of probability. *Monthly weather review*.
- BURLINA, P., JOSHI, N. and WANG, I. (2019). Where's wally now? deep generative and discriminative embeddings for novelty detection. In *CVPR*.
- CHALAPATHY, R. and CHAWLA, S. (2019). Deep learning for anomaly detection: A survey. *arXiv preprint arXiv:1901.03407*.
- CHANDOLA, V., BANERJEE, A. and KUMAR, V. (2007). Outlier detection: A survey. *ACM Computing Surveys*.
- CHANDOLA, V., BANERJEE, A. and KUMAR, V. (2009). Anomaly detection: A survey. *ACM computing surveys (CSUR)*.
- CHEN, J., SATHE, S., AGGARWAL, C. C. and TURAGA, D. S. (2017). Outlier detection with autoencoder ensembles. In *SDM*.

- CHEN, T., KORNBLITH, S., NOROUZI, M. and HINTON, G. E. (2020). A simple framework for contrastive learning of visual representations. In *ICML*.
- CHEN, Z., TIAN, Y., ZENG, W. and HUANG, T. (2015). Detecting abnormal behaviors in surveillance videos based on fuzzy clustering and multiple auto-encoders. In *ICME*.
- DUA, D. and GRAFF, C. (2017). UCI machine learning repository.
<http://archive.ics.uci.edu/ml>
- ESTER, M., KRIEGEL, H.-P., SANDER, J., XU, X. ET AL. (1996). A density-based algorithm for discovering clusters in large spatial databases with noise. In *KDD*.
- FEI-FEI, L., FERGUS, R. and PERONA, P. (2004). Learning generative visual models from few training examples: An incremental bayesian approach tested on 101 object categories. In *CVPRW*.
- FU, K., CHENG, D., TU, Y. and ZHANG, L. (2016). Credit card fraud detection using convolutional neural networks. In *International Conference on Neural Information Processing*.
- GIDARIS, S., SINGH, P. and KOMODAKIS, N. (2018). Unsupervised representation learning by predicting image rotations. In *ICLR*.
- GOLAN, I. and EL-YANIV, R. (2018). Deep anomaly detection using geometric transformations. In *NeurIPS*.
- GOODFELLOW, I. J., SHLENS, J. and SZEGEDY, C. (2014). Explaining and harnessing adversarial examples. In *ICLR*.
- GU, X., SUN, J. and XU, Z. (2020). Spherical space domain adaptation with robust pseudo-label loss. In *CVPR*.
- HE, K., ZHANG, X., REN, S. and SUN, J. (2016). Deep residual learning for image recognition. In *CVPR*.
- HE, Z., XU, X. and DENG, S. (2003). Discovering cluster-based local outliers. *Pattern Recognition Letters*.
- HENDRYCKS, D., MAZEIKA, M. and DIETTERICH, T. G. (2019). Deep anomaly detection with outlier exposure. In *ICLR*.
- HSU, Y.-C., SHEN, Y., JIN, H. and KIRA, Z. (2020). Generalized odin: Detecting out-of-distribution image without learning from out-of-distribution data. In *CVPR*.
- IOFFE, S. and SZEGEDY, C. (2015). Batch normalization: Accelerating deep network training by reducing internal covariate shift. In *ICML*.
- KHAN, S. and YAIRI, T. (2018). A review on the application of deep learning in system health management. *Mechanical Systems and Signal Processing*.
- KIM, J. and SCOTT, C. D. (2012). Robust kernel density estimation. *JMLR*.
- KINGMA, D. P. and BA, J. (2015). Adam: A method for stochastic optimization. In *ICLR*.
- KRIZHEVSKY, A., HINTON, G. ET AL. (2009). Learning multiple layers of features from tiny images.

- KUMAGAI, A., IWATA, T. and FUJIWARA, Y. (2019). Transfer anomaly detection by inferring latent domain representations. In *NeurIPS*.
- KWON, D., KIM, H., KIM, J., SUH, S. C., KIM, I. and KIM, K. J. (2019). A survey of deep learning-based network anomaly detection. *Cluster Computing*.
- KWON, G., PRABHUSHANKAR, M., TEMEL, D. and ALREGIB, G. (2020). Backpropagated gradient representations for anomaly detection. In *ECCV*.
- LAI, C., ZOU, D. and LERMAN, G. (2020a). Robust subspace recovery layer for unsupervised anomaly detection. In *ICLR*.
- LAI, C.-H., ZOU, D. and LERMAN, G. (2020b). Novelty detection via robust variational autoencoding. *arXiv preprint arXiv:2006.05534*.
- LANG, K. (1995). Newsweeder: Learning to filter netnews. In *Machine Learning Proceedings*.
- LEE, K., LEE, K., LEE, H. and SHIN, J. (2018). A simple unified framework for detecting out-of-distribution samples and adversarial attacks. In *NeurIPS*.
- LERMAN, G. and MAUNU, T. (2018). An overview of robust subspace recovery. *Proceedings of the IEEE*.
- LIANG, S., LI, Y. and SRIKANT, R. (2018). Enhancing the reliability of out-of-distribution image detection in neural networks. In *ICLR*.
- LIU, F. T., TING, K. M. and ZHOU, Z.-H. (2008). Isolation forest. In *ICDM*.
- LIU, W., WANG, X., OWENS, J. D. and LI, Y. (2020). Energy-based out-of-distribution detection. *arXiv preprint arXiv:2010.03759*.
- MIN, S., LEE, B. and YOON, S. (2017). Deep learning in bioinformatics. *Briefings in bioinformatics*.
- NAZARE, T. S., DE MELLO, R. F. and PONTI, M. A. (2018). Are pre-trained cnns good feature extractors for anomaly detection in surveillance videos? *arXiv preprint arXiv:1811.08495*.
- OORD, A. v. D., LI, Y. and VINYALS, O. (2018). Representation learning with contrastive predictive coding. *arXiv preprint arXiv:1807.03748*.
- PAFFENROTH, R., KAY, K. and SERVI, L. (2018). Robust pca for anomaly detection in cyber networks. *arXiv preprint arXiv:1801.01571*.
- PANG, G., SHEN, C., CAO, L. and HENGEL, A. v. D. (2020a). Deep learning for anomaly detection: A review. *arXiv preprint arXiv:2007.02500*.
- PANG, G., YAN, C., SHEN, C., VAN DEN HENGEL, A. and BAI, X. (2020b). Self-trained deep ordinal regression for end-to-end video anomaly detection. In *CVPR*.
- PEDREGOSA, F., VAROQUAUX, G., GRAMFORT, A., MICHEL, V., THIRION, B., GRISEL, O., BLONDEL, M., PRETTEHOFER, P., WEISS, R., DUBOURG, V. ET AL. (2011). Scikit-learn: Machine learning in python. *JMLR*.

- PERERA, P., NALLAPATI, R. and XIANG, B. (2019). OCGAN: one-class novelty detection using gans with constrained latent representations. In *CVPR*.
- PIDHORSKYI, S., ALMOHSEN, R. and DORETTO, G. (2018). Generative probabilistic novelty detection with adversarial autoencoders. In *NeurIPS*.
- RAJARAMAN, A. and ULLMAN, J. D. (2011). *Mining of massive datasets*. Cambridge University Press.
- REISS, T., COHEN, N., BERGMAN, L. and HOSHEN, Y. (2021). Panda: Adapting pretrained features for anomaly detection and segmentation. In *CVPR*.
- RIPPEL, O., MERTENS, P. and MERHOF, D. (2020). Modeling the distribution of normal data in pre-trained deep features for anomaly detection. *arXiv preprint arXiv:2005.14140*.
- RUFF, L., KAUFFMANN, J. R., VANDERMEULEN, R. A., MONTAVON, G., SAMEK, W., KLOFT, M., DIETTERICH, T. G. and MÜLLER, K.-R. (2020). A unifying review of deep and shallow anomaly detection. *arXiv preprint arXiv:2009.11732*.
- SABOKROU, M., FAYYAZ, M., FATHY, M., MOAYED, Z. and KLETTE, R. (2018). Deep-anomaly: Fully convolutional neural network for fast anomaly detection in crowded scenes. *CVIU*.
- SCHIRRMESTER, R. T., ZHOU, Y., BALL, T. and ZHANG, D. (2020). Understanding anomaly detection with deep invertible networks through hierarchies of distributions and features. *arXiv preprint arXiv:2006.10848*.
- SCHÖLKOPF, B., WILLIAMSON, R. C., SMOLA, A. J., SHAWE-TAYLOR, J. and PLATT, J. C. (2000). Support vector method for novelty detection. In *NeurIPS*.
- SEHWAG, V., CHIANG, M. and MITTAL, P. (2021). Ssd: A unified framework for self-supervised outlier detection. In *ICLR*.
- SHEN, A., TONG, R. and DENG, Y. (2007). Application of classification models on credit card fraud detection. In *2007 International conference on service systems and service management*. IEEE.
- SHYU, M.-L., CHEN, S.-C., SARINNAKORN, K. and CHANG, L. (2003). A novel anomaly detection scheme based on principal component classifier. Tech. rep., MIAMI UNIV CORAL GABLES FL DEPT OF ELECTRICAL AND COMPUTER ENGINEERING.
- SIMONYAN, K. and ZISSERMAN, A. (2015). Very deep convolutional networks for large-scale image recognition. In *ICLR*.
- SOMEPELLI, G., WU, Y., BALAJI, Y., VINZAMURI, B. and FEIZI, S. (2020). Unsupervised anomaly detection with adversarial mirrored autoencoders. *arXiv e-prints*.
- SULTANI, W., CHEN, C. and SHAH, M. (2018). Real-world anomaly detection in surveillance videos. In *CVPR*.
- TACK, J., MO, S., JEONG, J. and SHIN, J. (2020). Csi: Novelty detection via contrastive learning on distributionally shifted instances. In *NeurIPS*.
- TAN, S. C., TING, K. M. and LIU, F. T. (2011). Fast anomaly detection for streaming data. In *IJCAI*.

- VENKATARAMANAN, S., PENG, K.-C., SINGH, R. V. and MAHALANOBIS, A. (2019). Attention guided anomaly detection and localization in images. *arXiv preprint arXiv:1911.08616*.
- VERCRUYSSSEN, V., MEERT, W. and DAVIS, J. (2020). Transfer learning for anomaly detection through localized and unsupervised instance selection. In *AAAI*.
- WANG, S., ZENG, Y., LIU, X., ZHU, E., YIN, J., XU, C. and KLOFT, M. (2019). Effective end-to-end unsupervised outlier detection via inlier priority of discriminative network. In *NeurIPS*.
- XU, B., WANG, N., CHEN, T. and LI, M. (2015). Empirical evaluation of rectified activations in convolutional network. *arXiv preprint arXiv:1505.00853*.
- YANG, X., LATECKI, L. J. and POKRAJAC, D. (2009). Outlier detection with globally optimal exemplar-based gmm. In *SDM*.
- ZENATI, H., FOO, C. S., LECOAT, B., MANEK, G. and CHANDRASEKHAR, V. R. (2018). Efficient gan-based anomaly detection. *arXiv preprint arXiv:1802.06222*.
- ZONG, B., SONG, Q., MIN, M. R., CHENG, W., LUMEZANU, C., CHO, D. and CHEN, H. (2018). Deep autoencoding gaussian mixture model for unsupervised anomaly detection. In *ICLR*.

A Proofs

A.1 Proof of Proposition 1

Proof. We first prove $\mathbf{A}\mathcal{V}$ is still a linear subspace of \mathbb{R}^k .

Suppose \mathbf{y}_1 and \mathbf{y}_2 are two vectors in $\mathbf{A}\mathcal{V}$, then by definition there exist $\mathbf{x}_1, \mathbf{x}_2 \in \mathcal{V}$ s.t. $\mathbf{A}\mathbf{x}_1 = \mathbf{y}_1, \mathbf{A}\mathbf{x}_2 = \mathbf{y}_2$. Hence

$$\begin{aligned}\mathbf{y}_1 + \mathbf{y}_2 &= \mathbf{A}\mathbf{x}_1 + \mathbf{A}\mathbf{x}_2 \\ &= \mathbf{A}(\mathbf{x}_1 + \mathbf{x}_2).\end{aligned}\tag{2}$$

Considering $\mathbf{x}_1, \mathbf{x}_2 \in \mathcal{V}$ and \mathcal{V} is a linear subspace, we have $\mathbf{x}_1 + \mathbf{x}_2 \in \mathcal{V}$. Combining this with (2) we obtain

$$\mathbf{y}_1 + \mathbf{y}_2 \in \mathbf{A}\mathcal{V}.\tag{3}$$

For any $c \in \mathbb{R}$, $c\mathbf{y}_1 = c\mathbf{A}\mathbf{x}_1 = \mathbf{A}(c\mathbf{x}_1)$. As $\mathbf{x}_1 \in \mathcal{V}$ and \mathcal{V} is a linear subspace, we have $c\mathbf{x}_1 \in \mathcal{V}$, therefore we get

$$c\mathbf{y}_1 \in \mathbf{A}\mathcal{V}.\tag{4}$$

Combining (3) and (4) we conclude $\mathbf{A}\mathcal{V}$ is a linear subspace of \mathbb{R}^k .

Next we prove $\mathbf{A}\mathcal{U}$ is still a convex set in \mathbb{R}^k .

Suppose \mathbf{y}'_1 and \mathbf{y}'_2 are two vectors in $\mathbf{A}\mathcal{U}$, then by definition there exist $\mathbf{x}'_1, \mathbf{x}'_2 \in \mathcal{U}$ s.t. $\mathbf{A}\mathbf{x}'_1 = \mathbf{y}'_1, \mathbf{A}\mathbf{x}'_2 = \mathbf{y}'_2$. Hence for any $0 < \alpha < 1$, we have

$$\begin{aligned}\alpha\mathbf{y}'_1 + (1 - \alpha)\mathbf{y}'_2 &= \alpha\mathbf{A}\mathbf{x}'_1 + (1 - \alpha)\mathbf{A}\mathbf{x}'_2 \\ &= \mathbf{A}(\alpha\mathbf{x}'_1 + (1 - \alpha)\mathbf{x}'_2).\end{aligned}\tag{5}$$

Since \mathcal{U} is a convex set in \mathbb{R}^d and $\mathbf{x}'_1, \mathbf{x}'_2 \in \mathcal{U}$, we have $\alpha\mathbf{x}'_1 + (1 - \alpha)\mathbf{x}'_2 \in \mathcal{U}$. Then by (5) we get $\alpha\mathbf{y}'_1 + (1 - \alpha)\mathbf{y}'_2 \in \mathbf{A}\mathcal{U}$. Thereby we proved the convexity of set $\mathbf{A}\mathcal{U}$. \square

A.2 Proof of Theorem 1

Proof. For notational simplicity, we use $\|\cdot\|$ to denote L2 norm $\|\cdot\|_2$ and we denote $\mathbf{A}^{(m)} = (a_{ij})$ in the following. Some of the proof techniques are adapted from Johnson–Lindenstrauss lemma ([Arriaga and Vempala, 1999](#)). We first prove property (1).

Consider $\forall \mathbf{v} \in \mathbb{R}^d$, by our definition we have $\mathbf{v}^{(m)} = \mathbf{A}^{(m)}\mathbf{v}$, we have

$$\begin{aligned}&P\left(\|\mathbf{v}^{(m)}\|^2 \geq (1 + \epsilon)k\|\mathbf{v}\|^2\right) \\ &= P\left(\|\mathbf{A}^{(m)}\mathbf{v}\|^2 \geq (1 + \epsilon)k\|\mathbf{v}\|^2\right) \\ &= P\left(\frac{\|\mathbf{A}^{(m)}\mathbf{v}\|^2}{\|\mathbf{v}\|^2} \geq (1 + \epsilon)k\right).\end{aligned}\tag{6}$$

Let

$$W \triangleq \frac{\|\mathbf{A}^{(m)}\mathbf{v}\|^2}{\|\mathbf{v}\|^2},$$

and

$$w_i \triangleq \frac{\sum_j a_{ij}v_j}{\|\mathbf{v}\|},$$

it is straightforward that

$$W = \sum_{i=1}^k w_i^2.$$

Because $a_{ij} \sim \mathcal{N}(0, 1)$ and $\{a_{ij}\}$ are i.i.d., we have $w_i \sim \mathcal{N}(0, 1)$ and $\{w_i\}$ are i.i.d. Hence by (6), for any $\alpha > 0$, we have

$$\begin{aligned} & P\left(\|\mathbf{v}^{(m)}\|^2 \geq (1 + \epsilon)k\|\mathbf{v}\|^2\right) \\ &= P(W \geq (1 + \epsilon)k) \\ &= P\left(e^{\alpha W} \geq e^{(1 + \epsilon)k\alpha}\right) \\ &\stackrel{(i)}{\leq} \frac{\mathbb{E}\left(e^{\alpha W}\right)}{e^{(1 + \epsilon)k\alpha}} \\ &\stackrel{(ii)}{=} \frac{\prod_{i=1}^k \mathbb{E}\left(e^{\alpha w_i^2}\right)}{e^{(1 + \epsilon)k\alpha}} \\ &= \left(\frac{\mathbb{E}\left(e^{\alpha w_1^2}\right)}{e^{(1 + \epsilon)\alpha}}\right)^k, \end{aligned} \tag{7}$$

where (i) comes from Markov's inequality and (ii) uses the fact that $\{w_i\}$ are i.i.d.. Notice that when $0 \leq \alpha < \frac{1}{2}$ we have

$$\begin{aligned} \mathbb{E}\left(e^{\alpha w_1^2}\right) &= \int_{-\infty}^{\infty} e^{\alpha w_1^2} \frac{1}{\sqrt{2\pi}} e^{-\frac{w_1^2}{2}} dw_1 \\ &= \int_{-\infty}^{\infty} \frac{1}{\sqrt{2\pi}} e^{-\frac{w_1^2}{2}(1 - 2\alpha)} dw_1 \\ &= \frac{1}{\sqrt{1 - 2\alpha}} \int_{-\infty}^{\infty} \frac{\sqrt{1 - 2\alpha}}{\sqrt{2\pi}} e^{-\frac{w_1^2}{2}(1 - 2\alpha)} dw_1 \\ &\stackrel{(i)}{=} \frac{1}{\sqrt{1 - 2\alpha}}, \end{aligned} \tag{8}$$

where (i) uses the integral of random variable with distribution $\mathcal{N}\left(0, \frac{1}{1 - 2\alpha}\right)$. Now plugging (8) into (11), we get

$$P\left(\|\mathbf{v}^{(m)}\|^2 \geq (1 + \epsilon)k\|\mathbf{v}\|^2\right) \leq \left(\frac{e^{-2(1 + \epsilon)\alpha}}{1 - 2\alpha}\right)^{\frac{k}{2}}.$$

Take $\alpha = \frac{\epsilon}{2(1+\epsilon)}$, we have

$$\begin{aligned}
P\left(\|\mathbf{v}^{(m)}\|^2 \geq (1+\epsilon)k\|\mathbf{v}\|^2\right) &\leq \left((1+\epsilon)e^{-\epsilon}\right)^{\frac{k}{2}} \\
&= \left(e^{\log(1+\epsilon)-\epsilon}\right)^{\frac{k}{2}} \\
&\stackrel{(i)}{\leq} \left(e^{-\left(\frac{\epsilon^2}{2}-\frac{\epsilon^3}{3}\right)}\right)^{\frac{k}{2}} \\
&\leq e^{-\frac{k}{4}(\epsilon^2-\epsilon^3)},
\end{aligned} \tag{9}$$

where (i) employs inequality $\log(1+x) < x - \frac{x^2}{2} + \frac{x^3}{3}$.

Similarly, we have

$$\begin{aligned}
&P\left(\|\mathbf{v}^{(m)}\|^2 \leq (1-\epsilon)k\|\mathbf{v}\|^2\right) \\
&= P\left(W \leq (1-\epsilon)k\right) \\
&\leq P\left(e^{-\alpha W} \geq e^{-(1-\epsilon)\alpha k}\right) \\
&\leq \frac{\mathbb{E}\left(e^{-\alpha W}\right)}{e^{-(1-\epsilon)\alpha k}} \\
&= \frac{\prod_{i=1}^k \mathbb{E}\left(e^{-\alpha w_i^2}\right)}{e^{-(1-\epsilon)\alpha k}} \\
&= \left(\frac{\mathbb{E}\left(e^{-\alpha w_1^2}\right)}{e^{-(1-\epsilon)\alpha}}\right)^k \\
&= \left(\frac{e^{2(1-\epsilon)\alpha}}{1+2\alpha}\right)^{\frac{k}{2}}.
\end{aligned}$$

Take $\alpha = \frac{\epsilon}{2(1-\epsilon)}$, we obtain

$$\begin{aligned}
P\left(\|\mathbf{v}^{(m)}\|^2 \leq (1-\epsilon)k\|\mathbf{v}\|^2\right) &\leq \left((1-\epsilon)e^{\epsilon}\right)^{\frac{k}{2}} \\
&= \left(e^{\log(1-\epsilon)+\epsilon}\right)^{\frac{k}{2}} \\
&\leq \left(e^{-\frac{\epsilon^2}{2}+\frac{\epsilon^3}{3}}\right)^{\frac{k}{2}} \\
&\leq e^{-\frac{k}{4}(\epsilon^2-\epsilon^3)}.
\end{aligned} \tag{10}$$

Combining (9) and (10) and setting $e^{-\frac{k}{4}(\epsilon^2-\epsilon^3)} < \frac{\delta}{2}$, we have: when $k > \frac{4\log\frac{2}{\delta}}{\epsilon^2-\epsilon^3}$, with probability at least $1-\delta$,

$$(1-\epsilon)\|\mathbf{v}\|^2 \leq \frac{\|\mathbf{v}^{(m)}\|^2}{k} \leq (1+\epsilon)\|\mathbf{v}\|^2. \tag{11}$$

Now for any vectors $\mathbf{v}_i, \mathbf{v}_j \in \mathbb{R}^d$, substituting \mathbf{v} in (11) by $\mathbf{v}_i - \mathbf{v}_j$, we hereby proved property (1).

Next we prove the property (2).

For any index pair (i, j) , applying (11) to vectors $\mathbf{v}_1 + \mathbf{v}_2$ and $\mathbf{v}_1 - \mathbf{v}_2$, we have when $k > \frac{4 \log \frac{4}{\delta}}{\epsilon^2 - \epsilon^3}$, with probability at least $1 - \delta$,

$$k(1 - \epsilon) \|\mathbf{v}_i + \mathbf{v}_j\|^2 \leq \|\mathbf{v}_i^{(m)} + \mathbf{v}_j^{(m)}\|^2 \leq k(1 + \epsilon) \|\mathbf{v}_i + \mathbf{v}_j\|^2, \quad (12)$$

$$k(1 - \epsilon) \|\mathbf{v}_i - \mathbf{v}_j\|^2 \leq \|\mathbf{v}_i^{(m)} - \mathbf{v}_j^{(m)}\|^2 \leq k(1 + \epsilon) \|\mathbf{v}_i - \mathbf{v}_j\|^2. \quad (13)$$

Hence we have

$$\begin{aligned} \mathbf{v}_i^{(m)} \cdot \mathbf{v}_j^{(m)} &= \frac{\|\mathbf{v}_i^{(m)} + \mathbf{v}_j^{(m)}\|^2 - \|\mathbf{v}_i^{(m)} - \mathbf{v}_j^{(m)}\|^2}{4} \\ &\stackrel{(i)}{\geq} \frac{k(1 - \epsilon) \|\mathbf{v}_i + \mathbf{v}_j\|^2 - k(1 + \epsilon) \|\mathbf{v}_i - \mathbf{v}_j\|^2}{4} \\ &\stackrel{(ii)}{=} \frac{k}{4} \left(4\mathbf{v}_i \cdot \mathbf{v}_j - 2\epsilon (\|\mathbf{v}_i\|^2 + \|\mathbf{v}_j\|^2) \right) \\ &= k(\mathbf{v}_i \cdot \mathbf{v}_j - \epsilon), \end{aligned} \quad (14)$$

where (i) uses the left hand side of (12) and right hand side of (13), and (ii) utilizes $\|\mathbf{v}_i\| = \|\mathbf{v}_j\| = 1$ due to L2 normalization. Likewise, we get

$$\begin{aligned} \mathbf{v}_i^{(m)} \cdot \mathbf{v}_j^{(m)} &= \frac{\|\mathbf{v}_i^{(m)} + \mathbf{v}_j^{(m)}\|^2 - \|\mathbf{v}_i^{(m)} - \mathbf{v}_j^{(m)}\|^2}{4} \\ &\leq \frac{k(1 + \epsilon) \|\mathbf{v}_i + \mathbf{v}_j\|^2 - k(1 - \epsilon) \|\mathbf{v}_i - \mathbf{v}_j\|^2}{4} \\ &= \frac{k}{4} \left(4\mathbf{v}_i \cdot \mathbf{v}_j + 2\epsilon (\|\mathbf{v}_i\|^2 + \|\mathbf{v}_j\|^2) \right) \\ &= k(\mathbf{v}_i \cdot \mathbf{v}_j + \epsilon), \end{aligned} \quad (15)$$

Combining (14) and (15), we get as long as $k > \frac{4 \log \frac{4}{\delta}}{\epsilon^2 - \epsilon^3}$, with probability at least $1 - \delta$,

$$\mathbf{v}_i \cdot \mathbf{v}_j - \epsilon \leq \frac{\mathbf{v}_i^{(m)} \cdot \mathbf{v}_j^{(m)}}{k} \leq \mathbf{v}_i \cdot \mathbf{v}_j + \epsilon.$$

□

B Complete Results

In this section we provide the UAD performance comparison on image tasks using ResNet-101 as feature extractor. As illustrated above in Fig. 4, our methods still achieve the best performance consistently.

We also provide the detailed UAD performance results on CIFAR-10 and text tabular datasets. Note that our reported results in the main paper is the averaged AUROC and AUPR, as we have

Dataset	p	IF	OCSVM	DAGMM	RSRAE	PANDA	SLA (ours)	SLA ² P (ours)
CIFAR-10	0.1	85.44 / 45.60	87.30 / 50.23	64.27 / 19.60	84.33 / 45.95	88.68 / 60.11	<u>92.74</u> / <u>65.59</u>	94.08 / 73.62
	0.3	81.45 / 58.85	81.29 / 58.14	68.34 / 38.61	75.72 / 52.42	87.36 / 65.35	<u>90.08</u> / <u>74.93</u>	91.66 / 78.28
	0.5	78.65 / 64.72	76.32 / 60.83	68.68 / 50.61	72.06 / 58.15	83.06 / 71.27	<u>87.11</u> / <u>76.56</u>	89.18 / 80.69
CIFAR-100	0.1	79.12 / 34.93	81.69 / 37.44	53.52 / 11.95	91.40 / 60.68	87.90 / <u>58.41</u>	<u>89.94</u> / 58.38	93.04 / 75.05
	0.3	75.91 / 51.41	76.23 / 50.37	53.99 / 27.21	87.35 / 69.41	86.65 / 64.35	<u>87.63</u> / <u>71.31</u>	87.92 / 73.40
	0.5	73.29 / 58.90	72.35 / 56.26	55.36 / 39.21	84.12 / 72.61	81.81 / 69.62	85.36 / 75.37	<u>84.61</u> / <u>74.41</u>
Caltech 101	0.1	91.11 / 62.71	93.27 / 70.29	72.26 / 33.32	95.24 / 78.83	96.40 / 81.11	<u>96.69</u> / <u>82.87</u>	96.98 / 84.73
	0.3	87.41 / 70.92	88.60 / 74.02	74.01 / 51.49	89.47 / 73.90	95.16 / 88.38	<u>96.23</u> / <u>89.44</u>	96.48 / 90.94
	0.5	84.68 / 73.63	83.50 / 71.99	70.09 / 56.17	84.95 / 75.30	94.27 / 90.34	<u>94.89</u> / <u>90.40</u>	97.25 / 95.76

Table 4: AUROC/AUPR (%) results on image datasets for UAD with ResNet-101 as the feature extractor. The best in bold and the second best underlined. The mean scores over 5 independent runs are reported.

mentioned that in each dataset each class serves as normal data in turn. The 20 superclasses of CIFAR-100 are 'fish', 'flowers', 'food containers', 'fruit and vegetables', 'household electrical devices', 'household furniture', 'insects', 'large carnivores', 'large man-made outdoor things', 'large natural outdoor scenes', 'large omnivores and herbivores', 'medium-sized mammals', 'non-insect invertebrates', 'people', 'reptiles', 'small mammals', 'trees', 'vehicles' and 'vehicles 2'. The 11 selected classes of Caltech are 'watch', 'ketch', 'hawksbill', 'grand piano', 'chandelier', 'car side', 'bonsai', 'airplanes', 'motorbikes', 'leopards' and 'faces'. All the experiments are run 5 times independently using seeds 0, 1, 2, 3, 4, and averaged scores±standard deviations are reported.

Inlier class name	IF	OCSVM	DAGMM	E ³ Outlier	RSRAE	PANDA	SLA (ours)	SLA ² P (ours)
airplane	84.82±0.76	85.21±0.62	68.51±0.01	78.61±0.69	83.95±0.61	87.48±0.59	88.84±0.60	90.50±0.58
automobile	92.33±0.56	94.68±0.40	66.64±0.02	95.47±0.65	93.12±0.59	96.34±0.31	96.77±0.28	97.21±0.30
bird	74.39±0.88	72.87±1.01	46.31±0.01	79.08±0.61	72.90±1.63	77.77±0.97	81.30±1.19	83.83±1.33
cat	75.37±2.23	80.87±0.45	74.71±0.00	73.92±1.23	67.11±3.12	83.58±0.46	86.49±0.92	88.59±0.81
deer	87.01±1.24	87.88±0.26	76.41±0.04	84.91±1.01	84.94±1.57	90.87±0.34	90.65±0.38	92.13±0.44
dog	71.14±4.30	74.42±0.41	47.20±0.01	86.76±0.97	80.01±0.88	75.38±0.96	87.99±0.85	89.86±1.04
frog	87.02±0.60	86.23±0.79	76.09±0.02	87.21±0.63	81.87±2.14	86.59±0.58	91.68±0.37	93.05±0.39
horse	79.89±2.61	83.68±0.81	47.81±0.03	92.19±0.93	88.92±1.43	85.16±0.29	93.32±0.26	94.16±0.29
ship	89.47±1.31	91.23±0.20	78.24±5.61	92.62±0.51	89.91±1.71	90.06±0.47	94.64±0.50	95.76±0.48
truck	90.61±1.40	92.90±0.49	62.33±3.55	90.90±1.04	93.10±0.35	93.60±0.32	96.44±0.48	96.98±0.31
<i>average</i>	83.24±0.91	85.19±0.13	59.86±0.03	85.89±0.08	83.58±0.21	86.69±0.57	90.81±0.15	91.56±0.12

Table 5: AUROC (%) on CIFAR-10 for UAD using ResNet-50 as extractor when $p = 0.1$. The best performance is in bold.

Inlier class name	IF	OCSVM	DAGMM	E ³ Outlier	RSRAE	PANDA	SLA (ours)	SLA ² P (ours)
airplane	81.51±1.50	80.18±0.38	76.62±0.03	76.22±0.71	77.04±0.75	83.39±0.88	85.45±0.27	86.96±0.41
automobile	90.01±1.58	91.28±0.12	87.76±0.01	94.32±0.52	88.78±0.43	94.63±0.54	95.62±0.30	96.21±0.26
bird	67.18±1.28	67.23±0.53	67.29±0.01	71.18±2.39	62.03±1.48	73.37±2.11	76.36±0.53	77.66±0.38
cat	70.71±1.10	75.08±0.60	77.23±0.02	62.54±1.97	52.22±1.19	81.97±0.74	82.00±0.99	83.38±0.88
deer	84.11±0.18	83.12±0.29	82.01±0.04	80.76±1.36	76.23±1.86	88.46±0.62	88.16±0.47	89.73±0.58
dog	64.42±3.11	67.10±0.38	52.12±0.01	76.67±1.05	71.12±0.83	69.70±1.78	82.58±1.13	85.42±0.57
frog	83.13±1.53	78.79±0.51	75.78±0.02	80.33±2.00	69.91±2.19	82.36±0.82	87.46±0.54	89.75±0.52
horse	73.82±2.10	77.11±0.31	52.79±0.01	87.31±0.87	80.31±0.81	81.97±0.51	91.46±0.17	92.38±0.29
ship	85.73±1.76	85.85±0.38	72.72±18.01	90.52±1.21	84.04±1.19	88.63±0.73	92.51±0.17	93.85±0.33
truck	89.08±0.68	88.69±0.18	84.87±4.69	90.13±0.78	89.40±0.64	91.77±0.67	95.17±0.33	95.78±0.29
<i>average</i>	79.36±0.81	79.52±0.10	67.04±2.19	80.58±0.35	75.05±0.32	83.63±0.94	87.68±0.25	87.69±0.18

Table 6: AUROC (%) on CIFAR-10 for UAD using ResNet-50 as extractor when $p = 0.3$. The best performance is in bold.

Inlier class name	IF	OCSVM	DAGMM	E ³ Outlier	RSRAE	PANDA	SLA (ours)	SLA ² P (ours)
airplane	79.51±1.78	75.67±0.42	79.02±3.22	73.79±1.01	73.68±0.51	83.61±1.15	81.76±0.43	84.17±1.14
automobile	87.57±1.39	86.88±0.28	86.11±0.02	93.32±0.54	86.02±0.87	92.92±0.77	94.38±0.44	95.31±0.33
bird	65.67±2.08	63.29±0.43	72.02±2.41	65.53±2.19	57.62±0.87	72.25±2.37	72.76±0.69	73.20±0.79
cat	67.61±2.60	71.20±0.43	78.35±2.03	55.78±1.70	48.51±1.41	79.67±1.24	77.74±0.40	79.95±0.18
deer	82.13±1.56	79.14±0.15	77.44±2.31	76.01±1.41	72.58±1.28	88.24±0.96	85.74±0.47	88.04±0.33
dog	59.58±3.01	62.38±0.18	59.76±0.28	72.12±3.14	63.19±0.76	70.48±2.12	77.76±0.85	81.12±1.14
frog	80.52±1.11	73.02±0.45	85.67±7.02	74.59±0.73	64.81±1.00	79.89±1.18	81.83±0.64	85.26±1.69
horse	71.08±1.37	72.17±0.16	53.93±11.51	85.38±1.04	78.03±1.12	80.92±0.95	90.16±0.26	91.50±0.40
ship	83.20±1.91	80.62±0.33	84.14±1.97	89.51±0.58	80.42±0.89	89.22±1.38	90.12±0.42	92.38±0.41
truck	86.32±0.89	83.29±0.07	75.03±11.55	87.58±0.78	87.02±0.44	90.32±0.74	94.17±0.25	95.35±0.54
<i>average</i>	75.94±0.91	74.83±0.14	62.73±0.81	77.44±0.62	71.27±0.33	82.75±1.11	84.64±0.10	84.71±0.27

Table 7: AUROC (%) on CIFAR-10 for UAD using ResNet-50 as extractor when $p = 0.5$. The best performance is in bold.

Dataset	Inlier class name	IF	OCSVM	DAGMM	RSRAE	SLA (ours)	SLA ² P (ours)
20 Newsgroups	alt.atheism	55.29±3.70	95.59±0.00	59.36±3.59	94.52±1.24	96.11±0.19	96.20±0.34
	comp.graphics	68.14±2.53	65.23±0.00	58.41±3.04	84.23±2.55	83.73±0.71	88.62±0.33
	comp.os.ms-windows.misc	64.75±1.71	82.64±0.00	56.84±4.48	88.45±2.51	89.35±0.87	91.98±0.27
	comp.sys.ibm.pc.hardware	63.77±2.39	73.21±0.00	61.36±5.04	84.36±5.44	86.89±0.90	90.16±0.14
	comp.sys.mac.hardware	60.83±2.33	73.96±0.00	56.03±2.13	88.69±2.80	88.06±0.68	91.86±0.21
	comp.windows.x	65.17±5.17	69.78±0.00	54.70±5.14	86.52±1.91	91.21±0.50	94.07±0.30
	misc.forsale	67.01±1.57	73.47±0.00	58.39±5.40	86.99±4.28	85.76±0.82	90.74±0.53
	rec.autos	55.60±3.88	70.76±0.00	57.86±5.02	87.45±4.69	88.33±0.97	91.46±0.38
	rec.motorcycles	52.12±4.00	87.94±0.00	54.78±3.63	92.51±1.90	93.40±0.50	95.66±0.23
	rec.sport.baseball	62.46±2.82	82.73±0.00	61.20±3.65	91.39±1.68	92.91±0.37	95.29±0.18
	rec.sport.hockey	59.82±2.13	92.38±0.00	53.36±10.76	94.98±0.99	95.75±0.47	97.12±0.14
	sci.crypt	46.89±2.39	93.50±0.00	61.73±2.82	97.23±0.55	95.58±0.29	96.14±0.14
	sci.electronics	59.80±2.38	61.22±0.00	58.41±4.79	76.29±3.05	79.99±1.03	86.73±0.38
	sci.med	56.97±2.58	77.48±0.00	47.21±5.49	83.93±0.95	89.64±0.22	91.89±0.48
	sci.space	53.04±3.65	87.06±0.00	48.34±4.43	90.84±1.93	92.81±0.39	93.71±0.24
	soc.religion.christian	51.60±3.59	91.81±0.00	51.52±8.33	90.45±1.72	93.00±0.35	94.38±0.26
	talk.politics.guns	49.52±2.51	92.25±0.00	56.55±7.24	92.67±1.67	93.42±0.29	95.44±0.12
	talk.politics.mideast	43.62±3.10	96.00±0.00	45.74±6.15	94.92±2.20	96.71±0.14	97.53±0.12
talk.politics.misc	43.73±2.04	86.44±0.00	48.90±6.42	90.04±1.24	91.84±0.41	93.20±0.29	
talk.religion.misc	48.89±5.79	87.45±0.00	46.01±5.13	84.17±3.43	90.84±0.35	91.89±0.17	
	<i>average</i>	56.45±0.67	82.04±0.00	54.84±2.27	89.03±2.34	90.77±0.12	93.20±0.07
Reuters-21578	exchanges	75.79±0.94	96.81±0.00	77.35±7.09	96.66±1.34	96.89±0.25	98.27±0.12
	organizations	66.01±3.94	69.98±0.00	62.53±5.03	76.50±4.25	80.73±0.31	86.72±0.57
	people	58.43±3.70	97.81±0.00	63.61±8.67	95.67±0.14	97.77±0.08	98.23±0.15
	places	52.74±1.89	96.70±0.00	59.74±7.47	96.47±2.09	97.12±0.07	97.93±0.11
	topics	43.53±3.31	93.46±0.00	62.11±8.28	96.90±0.70	95.03±0.24	97.71±0.08
		<i>average</i>	59.30±0.82	90.95±0.00	65.07±4.12	92.44±1.70	93.51±0.09

Table 8: AUROC (%) on text datasets for UAD when $p = 0.1$. The best performance is in bold.

Dataset	Inlier class name	IF	OCSVM	DAGMM	RSRAE	SLA (ours)	SLA ² P (ours)
20 Newsgroups	alt.atheism	12.41±0.30	78.86±0.00	13.12±1.92	73.39±3.24	79.37±1.62	83.86±0.93
	comp.graphics	18.61±1.73	18.66±0.00	14.40±2.31	36.56±5.32	31.62±3.30	63.21±1.62
	comp.os.ms-windows.misc	16.01±0.77	34.31±0.00	11.70±1.42	40.66±5.97	43.19±3.50	67.91±1.50
	comp.sys.ibm.pc.hardware	21.65±1.63	26.66±0.00	18.60±4.95	35.72±9.73	37.26±2.86	64.24±1.50
	comp.sys.mac.hardware	21.46±3.09	28.15±0.00	13.96±6.04	41.90±9.32	37.85±3.00	69.89±0.62
	comp.windows.x	16.19±2.55	19.63±0.00	13.50±4.18	36.58±2.78	40.45±3.01	66.94±0.88
	misc.forsale	23.36±1.56	29.37±0.00	15.40±3.30	45.05±6.36	35.80±3.90	65.81±2.33
	rec.autos	14.24±0.78	29.01±0.00	16.74±8.13	41.00±9.34	39.49±3.19	65.68±1.22
	rec.motorcycles	13.65±2.01	62.64±0.00	13.33±2.48	68.45±5.61	67.31±3.54	78.87±1.11
	rec.sport.baseball	16.72±1.20	50.43±0.00	13.77±2.66	54.76±3.15	55.98±1.14	76.46±1.14
	rec.sport.hockey	17.89±0.74	54.61±0.00	14.66±7.16	63.95±4.02	60.47±2.78	78.86±0.82
	sci.crypt	9.45±0.77	64.29±0.00	13.91±1.25	72.41±3.19	67.49±1.77	78.35±0.67
	sci.electronics	22.18±2.45	17.22±0.00	13.66±3.73	26.17±2.08	26.27±4.36	57.72±0.63
	sci.med	12.97±1.28	34.09±0.00	9.07±1.22	36.44±2.60	43.05±3.53	66.93±0.68
	sci.space	11.58±1.85	48.89±0.00	9.58±2.61	48.53±4.43	55.44±3.65	73.91±0.65
	soc.religion.christian	12.45±0.73	49.12±0.00	11.03±1.98	49.60±3.50	48.09±2.01	70.85±1.19
	talk.politics.guns	10.80±0.87	64.36±0.00	12.34±4.22	58.73±4.68	66.14±1.67	77.53±0.40
	talk.politics.mideast	9.51±1.56	67.09±0.00	9.59±2.47	68.82±8.68	70.68±1.24	83.68±1.30
talk.politics.misc	9.83±0.88	52.73±0.00	8.58±1.22	56.43±4.94	53.83±2.23	72.10±0.55	
talk.religion.misc	10.92±1.26	46.30±0.00	8.21±0.93	40.69±6.71	51.59±1.56	70.65±0.77	
	<i>average</i>	15.09±0.22	43.82±0.00	12.76±1.06	49.79±5.28	50.57±0.65	71.77±0.34
Reuters-21578	exchanges	36.21±0.64	71.23±0.00	38.72±11.34	73.37±9.35	71.77±3.63	87.68±1.00
	organizations	25.86±4.09	20.11±0.00	18.23±5.66	32.19±6.35	34.19±0.78	60.47±0.87
	people	11.94±1.39	71.16±0.00	17.14±5.29	67.57±4.98	71.39±1.83	85.48±0.86
	places	11.85±1.38	68.71±0.00	15.65±5.04	70.04±6.79	68.31±3.35	85.00±0.92
	topics	7.82±0.45	77.23±0.00	21.93±12.22	79.04±6.10	77.26±1.53	88.35±0.82
		<i>average</i>	18.74±0.93	61.69±0.00	22.33±3.62	64.44±6.71	64.58±1.34

Table 9: AUPR (%) on text datasets for UAD when $p = 0.1$. The best performance is in bold.

Dataset	Inlier class name	IF	OCSVM	DAGMM	RSRAE	SLA (ours)	SLA ² P (ours)
20 Newsgroups	alt.atheism	56.28±1.11	88.77±0.00	58.88±8.15	94.79±0.83	94.01±0.20	95.36±0.19
	comp.graphics	67.45±1.50	64.61±0.00	56.44±3.78	81.69±1.27	78.01±0.84	85.31±0.78
	comp.os.ms-windows.misc	65.54±3.20	75.41±0.00	58.71±4.46	88.43±0.72	86.04±0.31	89.69±0.30
	comp.sys.ibm.pc.hardware	66.70±2.86	67.15±0.00	54.50±2.96	84.51±1.28	81.46±0.85	86.95±0.93
	comp.sys.mac.hardware	66.15±1.20	67.72±0.00	56.47±2.82	87.35±1.71	82.56±0.49	88.18±0.41
	comp.windows.x	64.89±1.87	63.71±0.00	56.31±1.03	84.89±0.82	81.89±0.53	87.55±0.32
	misc.forsale	66.26±2.01	64.54±0.00	59.40±4.67	86.67±1.01	78.77±0.83	85.26±0.74
	rec.autos	57.95±1.62	69.99±0.00	51.62±3.82	86.59±1.73	83.80±0.43	88.41±0.55
	rec.motorcycles	57.71±1.11	73.54±0.00	50.54±3.15	92.41±1.00	89.02±0.41	92.45±0.31
	rec.sport.baseball	64.57±2.06	72.12±0.00	58.86±2.88	90.86±1.92	88.19±0.59	91.75±0.34
	rec.sport.hockey	61.35±1.78	85.87±0.00	56.12±3.93	94.25±0.95	92.45±0.49	94.44±0.41
	sci.crypt	53.63±1.62	90.63±0.00	55.95±5.21	96.89±0.32	93.59±0.19	94.88±0.20
	sci.electronics	59.84±2.64	57.25±0.00	54.57±3.14	77.03±2.45	72.75±0.11	80.84±0.36
	sci.med	55.63±1.61	71.56±0.00	47.53±2.51	83.20±1.87	84.28±0.71	88.71±0.61
	sci.space	54.62±1.82	77.32±0.00	53.03±7.49	91.16±0.98	89.11±0.16	91.80±0.25
	soc.religion.christian	52.36±2.13	82.46±0.00	61.11±5.88	90.11±1.59	87.99±0.44	90.39±0.47
	talk.politics.guns	48.15±1.56	83.58±0.00	52.52±5.13	92.55±0.88	91.46±0.19	93.57±0.32
	talk.politics.mideast	47.20±3.43	86.40±0.00	43.65±5.28	95.30±1.19	93.39±0.31	94.94±0.21
talk.politics.misc	47.73±3.22	80.08±0.00	47.48±4.14	91.81±1.58	89.22±0.40	91.84±0.34	
talk.religion.misc	52.96±1.35	78.64±0.00	47.62±2.46	86.63±1.93	87.86±0.14	90.87±0.21	
	<i>average</i>	58.35±0.45	75.07±0.00	54.07±0.57	88.86±1.30	86.29±0.11	90.16±0.11
Reuters-21578	exchanges	76.45±1.50	90.49±0.00	71.75±5.28	95.18±0.44	95.27±0.15	97.06±0.22
	organizations	67.49±3.11	57.04±0.00	60.68±4.51	63.66±2.88	60.48±0.32	89.91±0.75
	people	58.40±2.89	89.15±0.00	52.18±6.94	93.75±1.22	94.72±0.16	96.78±0.12
	places	48.81±2.12	88.10±0.00	56.93±5.25	94.64±1.00	94.82±0.10	97.06±0.16
	topics	43.18±2.63	91.41±0.00	55.11±8.95	96.25±0.49	95.04±0.16	96.79±0.17
		<i>average</i>	58.86±0.74	83.24±0.00	59.33±2.68	88.70±1.21	88.07±0.07

Table 10: AUROC (%) on text datasets for UAD when $p = 0.3$. The best performance is in bold.

Dataset	Inlier class name	IF	OCSVM	DAGMM	RSRAE	SLA (ours)	SLA ² P (ours)
20 Newsgroups	alt.atheism	32.34±1.21	79.18±0.00	30.32±7.71	87.05±1.62	85.45±1.17	89.27±0.87
	comp.graphics	38.58±0.91	32.30±0.00	29.75±3.33	51.82±1.83	47.93±1.08	64.49±1.70
	comp.os.ms-windows.misc	35.88±2.29	45.57±0.00	28.80±3.46	64.87±1.82	58.19±0.98	70.33±0.46
	comp.sys.ibm.pc.hardware	46.80±3.94	38.06±0.00	28.80±1.53	57.72±1.67	52.38±0.87	67.26±1.83
	comp.sys.mac.hardware	45.69±1.99	39.99±0.00	29.23±1.27	62.98±4.59	55.00±1.39	69.85±1.06
	comp.windows.x	37.76±1.25	34.38±0.00	26.95±0.41	56.12±2.17	51.28±0.98	66.50±0.79
	misc.forsale	44.86±2.90	38.19±0.00	32.07±3.83	63.22±1.39	50.60±1.76	66.44±1.98
	rec.autos	34.70±1.98	44.40±0.00	24.94±2.31	61.43±3.65	56.68±1.01	68.83±1.00
	rec.motorcycles	36.40±1.00	58.58±0.00	24.22±1.81	80.87±2.31	73.08±1.46	82.14±0.62
	rec.sport.baseball	38.35±3.57	51.58±0.00	30.98±3.30	74.09±4.16	68.20±1.85	77.87±0.79
	rec.sport.hockey	38.20±1.91	63.70±0.00	31.01±3.55	78.36±2.29	73.33±2.04	81.09±1.77
	sci.crypt	27.95±0.82	74.10±0.00	28.50±5.65	87.00±0.81	78.60±0.44	83.25±0.54
	sci.electronics	40.90±2.68	32.59±0.00	29.02±3.64	47.55±3.10	41.80±0.81	57.49±1.23
	sci.med	29.88±1.91	47.39±0.00	22.64±2.18	55.24±4.00	57.41±1.62	70.40±2.01
	sci.space	28.94±1.02	55.17±0.00	25.43±4.01	68.36±1.66	68.30±1.12	77.34±1.41
	soc.religion.christian	30.78±1.47	56.53±0.00	33.81±8.10	70.18±2.76	62.88±1.52	71.69±2.08
	talk.politics.guns	25.36±1.23	67.53±0.00	25.25±5.08	77.79±1.58	76.87±0.33	83.04±0.51
	talk.politics.mideast	23.78±1.88	67.66±0.00	20.52±2.50	83.25±3.11	77.06±0.81	82.88±0.67
talk.politics.misc	25.65±1.41	62.98±0.00	22.17±3.27	77.70±3.04	70.95±1.33	78.71±1.49	
talk.religion.misc	28.43±1.25	55.68±0.00	23.20±2.12	66.59±2.39	65.63±0.53	75.39±0.70	
	<i>average</i>	34.56±0.72	52.28±0.00	27.38±0.82	68.61±2.50	63.58±0.09	74.21±0.17
Reuters-21578	exchanges	57.39±3.64	71.58±0.00	51.14±8.66	83.75±2.41	81.89±0.87	90.39±0.48
	organizations	49.37±1.98	28.15±0.00	33.60±4.60	36.99±4.06	31.43±0.88	84.52±1.07
	people	26.28±2.34	69.27±0.00	27.53±4.12	78.52±2.78	79.64±1.30	90.09±0.41
	places	26.17±1.90	67.45±0.00	28.68±3.25	78.66±2.17	79.17±1.36	90.67±0.65
	topics	20.71±1.80	79.80±0.00	27.12±6.92	87.45±1.56	87.62±0.75	92.73±0.39
		<i>average</i>	35.99±0.70	63.25±0.00	33.61±2.77	73.07±2.60	71.95±0.42

Table 11: AUPR (%) on text datasets for UAD when $p = 0.3$. The best performance is in bold.

Dataset	Inlier class name	IF	OCSVM	DAGMM	RSRAE	SLA (ours)	SLA ² P (ours)
20 Newsgroups	alt.atheism	55.37±2.51	84.37±0.00	56.22±6.82	93.74±0.65	92.45±0.16	93.29±0.10
	comp.graphics	66.44±2.36	55.84±0.00	52.66±5.06	77.90±1.89	75.69±0.61	79.34±0.43
	comp.os.ms-windows.misc	67.75±2.34	68.66±0.00	54.80±6.22	86.54±0.82	84.54±0.36	86.62±0.37
	comp.sys.ibm.pc.hardware	65.91±1.58	65.63±0.00	59.71±4.35	82.21±1.60	79.41±0.57	82.21±0.45
	comp.sys.mac.hardware	66.34±1.31	63.12±0.00	56.00±2.59	85.15±1.24	80.53±0.47	82.87±0.27
	comp.windows.x	63.82±1.15	61.06±0.00	55.17±2.02	81.52±1.27	78.96±0.18	81.92±0.36
	misc.forsale	67.50±1.99	62.82±0.00	52.94±2.67	82.16±0.72	76.11±0.42	79.49±0.40
	rec.autos	55.86±1.07	70.15±0.00	49.91±3.20	84.62±1.59	81.96±0.62	84.40±0.37
	rec.motorcycles	55.01±0.55	70.27±0.00	52.22±3.01	89.93±2.14	86.92±0.31	88.64±0.35
	rec.sport.baseball	61.85±2.65	69.67±0.00	56.25±6.17	88.45±1.81	86.01±0.27	87.81±0.19
	rec.sport.hockey	59.34±2.73	76.95±0.00	59.53±3.58	92.81±0.88	90.10±0.15	91.25±0.12
	sci.crypt	51.13±1.73	83.21±0.00	52.09±10.96	96.29±0.32	92.63±0.11	93.48±0.17
	sci.electronics	59.41±2.32	59.95±0.00	49.29±3.30	73.16±2.59	71.19±0.36	75.72±0.39
	sci.med	55.23±2.43	64.81±0.00	46.71±5.30	80.61±1.20	81.55±0.38	84.00±0.29
	sci.space	52.55±1.61	74.08±0.00	48.36±3.08	89.45±0.70	87.76±0.41	89.27±0.24
	soc.religion.christian	50.07±0.92	78.20±0.00	57.08±5.01	89.15±1.60	87.14±0.31	88.78±0.31
	talk.politics.guns	44.45±1.68	80.81±0.00	46.17±5.30	91.27±1.20	90.20±0.32	91.44±0.17
	talk.politics.mideast	46.62±2.87	82.79±0.00	46.96±4.29	94.02±1.08	91.90±0.18	92.80±0.13
talk.politics.misc	45.09±2.11	78.98±0.00	40.78±2.39	89.48±1.47	88.45±0.19	89.48±0.23	
talk.religion.misc	50.29±2.74	75.32±0.00	45.86±6.69	86.11±1.46	86.14±0.49	88.13±0.38	
	<i>average</i>	57.00±0.33	71.33±0.00	51.94±1.02	86.73±1.31	84.48±0.11	86.55±0.06
Reuters-21578	exchanges	74.68±2.24	80.03±0.00	67.68±5.85	92.53±1.68	91.76±0.23	93.83±0.22
	organizations	65.09±1.57	48.58±0.00	62.84±4.04	51.99±2.66	46.62±0.33	55.99±0.54
	people	53.49±3.23	79.78±0.00	60.71±5.49	89.64±3.78	91.05±0.15	93.25±0.16
	places	48.26±1.21	79.49±0.00	60.54±4.41	87.54±5.76	90.53±0.14	92.54±0.12
	topics	37.70±2.64	86.50±0.00	58.30±9.01	95.27±0.43	94.41±0.17	94.84±0.18
		<i>average</i>	55.85±0.87	74.88±0.00	62.01±2.54	83.39±2.86	82.87±0.06

Table 12: AUROC (%) on text datasets for UAD when $p = 0.5$. The best performance is in bold.

Dataset	Inlier class name	IF	OCSVM	DAGMM	RSRAE	SLA (ours)	SLA ² P (ours)
20 Newsgroups	alt.atheism	41.80±1.28	79.72±0.00	38.23±5.56	89.16±0.83	88.14±0.76	90.11±0.50
	comp.graphics	50.38±1.99	39.35±0.00	36.54±3.53	58.07±1.96	57.25±1.74	68.75±0.90
	comp.os.ms-windows.misc	49.54±1.91	51.78±0.00	37.20±4.28	69.13±1.55	68.15±0.86	75.75±0.64
	comp.sys.ibm.pc.hardware	55.09±1.86	49.65±0.00	44.41±4.83	64.54±3.11	61.92±0.97	71.14±0.72
	comp.sys.mac.hardware	56.40±1.03	48.76±0.00	40.85±4.84	70.01±1.79	64.67±1.25	72.49±0.53
	comp.windows.x	48.97±0.93	44.21±0.00	38.15±1.59	61.97±2.37	60.07±1.12	71.15±0.69
	misc.forsale	55.78±2.54	46.97±0.00	37.19±3.33	66.20±1.36	58.45±1.07	69.10±0.81
	rec.autos	42.72±1.51	56.07±0.00	32.65±2.24	68.25±2.42	66.11±1.85	74.91±0.90
	rec.motorcycles	44.48±1.12	63.35±0.00	35.54±2.10	82.33±2.47	78.90±1.05	82.95±0.73
	rec.sport.baseball	46.19±1.98	57.15±0.00	39.12±6.25	77.70±3.58	74.16±1.01	80.34±0.42
	rec.sport.hockey	46.73±3.28	64.72±0.00	42.38±2.78	83.08±1.32	78.62±0.50	83.97±0.37
	sci.crypt	36.27±1.20	74.18±0.00	35.10±6.49	89.82±0.55	84.09±0.89	88.19±0.40
	sci.electronics	51.65±3.19	45.37±0.00	33.21±2.73	54.24±2.96	53.56±0.72	64.96±0.66
	sci.med	39.89±1.90	51.69±0.00	32.02±3.27	63.48±1.64	65.62±0.45	73.90±0.45
	sci.space	37.12±1.18	59.51±0.00	32.97±2.01	75.09±2.18	76.06±1.13	81.51±0.61
	soc.religion.christian	37.47±1.58	62.21±0.00	40.12±6.40	76.40±2.17	71.70±1.39	78.83±0.63
	talk.politics.guns	32.83±1.22	72.04±0.00	30.75±3.50	82.08±2.11	81.78±0.36	85.33±0.13
	talk.politics.mideast	32.75±2.12	71.31±0.00	31.91±1.96	85.94±2.04	81.87±0.33	86.19±0.22
talk.politics.misc	33.10±2.06	69.18±0.00	27.86±1.10	80.16±2.93	78.86±0.40	82.97±0.47	
talk.religion.misc	36.14±2.19	62.59±0.00	32.33±3.58	73.37±2.50	73.69±1.48	80.12±0.77	
	<i>average</i>	43.77±0.21	58.49±0.00	35.93±0.62	73.55±2.09	71.18±0.22	78.13±0.11
Reuters-21578	exchanges	62.72±2.18	66.11±0.00	55.81±7.96	83.71±3.17	80.48±0.89	87.02±0.48
	organizations	53.76±3.25	34.05±0.00	44.81±4.25	38.47±2.70	33.05±0.21	49.14±0.63
	people	34.28±2.33	67.09±0.00	44.57±7.30	78.33±6.13	80.38±0.66	86.85±0.40
	places	33.34±0.93	66.53±0.00	44.53±5.87	74.31±8.89	79.54±0.84	85.62±0.31
	topics	26.38±1.08	78.00±0.00	43.00±9.53	89.82±0.51	89.74±0.35	90.97±0.30
		<i>average</i>	42.10±0.92	62.36±0.00	46.54±2.09	72.93±4.28	72.64±0.15

Table 13: AUPR (%) on text datasets for UAD when $p = 0.5$. The best performance is in bold.